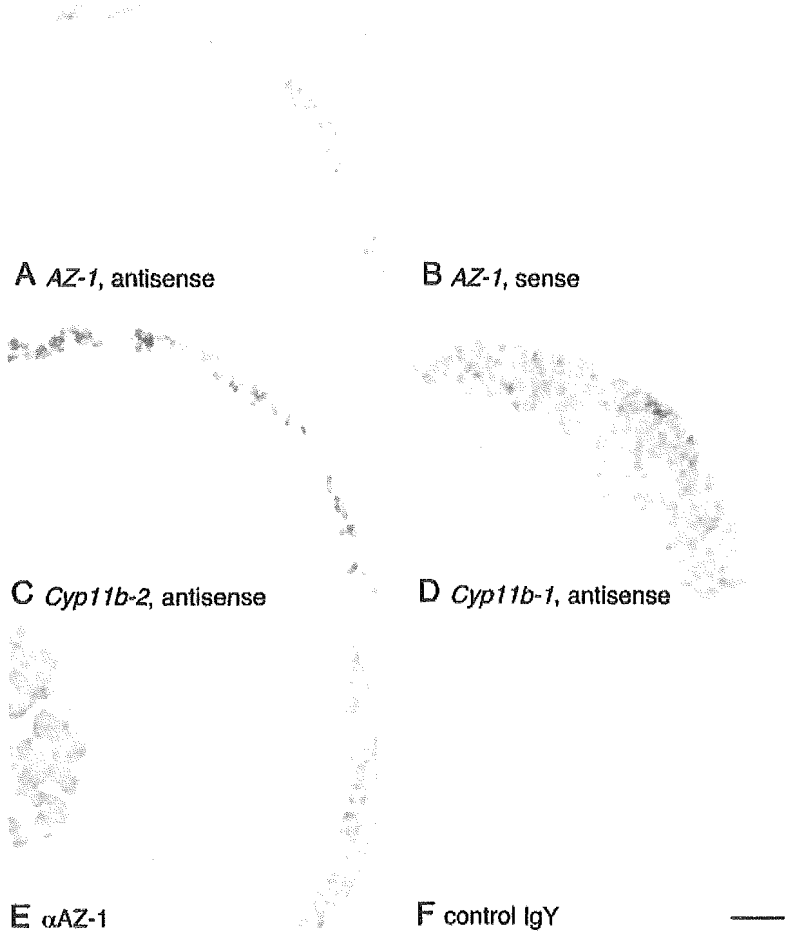

FIG. 5. **Localization of mouse AZ-1 in the adrenal glands.** *A, in situ* hybridization analysis of mouse adrenal sections using DIG-labeled AZ-1 antisense RNA probe shows *dark purple* staining in the outer cortical regions composed of zG and zU and the medulla. Note that AZ-1 mRNA signals are detectable in zG irrespective of Cyp11b-2 mRNA expression and in zU (compare with the hybridization signals in *C* and *D*). *B, in situ* hybridization using labeled AZ-1 sense RNA probe gives a weak background signal comparable with that detectable with the antisense probe. *C, in situ* hybridization using the labeled Cyp11b-2 antisense RNA probe shows hybridization signals sporadically in zG. *D, in situ* hybridization using the labeled Cyp11b-1 antisense RNA probe shows hybridization signals in zFR. *E*, immunohistochemistry using the affinity-purified chicken anti-AZ-1 antibody shows *reddish brown* staining in the outer cortical regions composed of zG and zU and the medulla. Distribution of AZ-1 immunoreactivity is comparable with that of AZ-1 mRNA (compare with the signals in *A*). *F*, immunohistochemistry using a control chicken IgY gives a weak background signal comparable with that seen with anti-AZ-1 antibody. *Bar*, 50 μm.

established simultaneously with AcA101 and AcA201 were also analyzed for AZ-1 mRNA. Levels of the mRNA in such cell lines as AcE60 (25) were consistent with their phenotypes; cell lines displaying functionally undifferentiated phenotypes had higher levels of AZ-1 mRNA expression than those displaying differentiated ones (data not shown).

RNA preparations from various organs of mouse were then analyzed by Northern blot analysis using AZ-1 cDNA as the probe (Fig. 4*B*). The greatest hybridization signal was obtained with RNA from adrenal glands (*lane 5*) among the organs examined in the experiments. Although AZ-1 mRNA was undetectable in the whole brain (*lane 4*), it was detectable in other organs as follows: heart (*lane 6*), skeletal muscle (*lane 7*), kidney (*lane 8*), liver (*lane 9*), and spleen (*lane 10*). Despite the ability to execute steroidogenesis, testis gave no hybridization signal (*lane 11*).

Subsequently, *in situ* hybridization analysis was performed to locate expression of AZ-1 mRNA in the adrenal glands. As shown in Fig. 5*A*, hybridization signals of an antisense probe for AZ-1 mRNA were detected in the outer cortical regions composed of zG and zU. The medulla also exhibited weak hybridization signals. Nuclei of the zF cells appeared to give weak nonspecific signals. The faint signals seen in the FR were nonspecific background comparable with those detected with the sense probe (Fig. 5*B*). To compare the location of AZ-1 mRNA with those of Cyp11b-2 mRNA, *in situ* hybridization employing an antisense probe for Cyp11b-2 was performed. Cyp11b-2 mRNA was observed sporadically in zG (Fig. 5*C*). It should thus be noted that AZ-1 mRNA signals were detectable irrespective of the hybridization signals for Cyp11b-2 mRNA in zG. When an antisense probe for Cyp11b-1 was used, hybridization signals were detected in zFR (Fig. 5*D*). As shown, the hybridization signals for AZ-1 mRNA (Fig. 5*A*) and those for Cyp11b-1 mRNA (Fig. 5*D*) did not overlap each other. Therefore, AZ-1 mRNA signals were present in zG and zU but not in zFR, which express Cyp11b-1 mRNA.

Fig. 5*E* illustrates immunohistochemical localization of the AZ-1 protein in mouse adrenal glands by using an anti-AZ-1 antibody raised against peptide antigens (see "Experimental Procedures"). The immunoreactivities were detected in the outer cortical regions corresponding to zG and zU. The weak signals in zFR seemed to be nonspecific because the control IgY gave a comparable level of background (Fig. 5*F*). The medulla was also immunoreactive. Thus, distribution of the immunoreactivities to anti-AZ-1 antibody and that of the hybridization signals of the AZ-1 antisense probe were indistinguishable from each other. Both AZ-1 mRNA and protein were thus expressed in the outer regions of the adrenal cortex, *i.e.* the outside of zFR.

Detection of FLAG-tagged AZ-1 Protein with Stably Transfected Y-1 Cells—We then produced stable transfectants of Y-1 cells with an expression vector encoding AZ-1F protein. Among the clones obtained, a clone exhibiting the highest expression level of AZ-1F mRNA was characterized in detail. When the cell extracts prepared from the clone were analyzed by immunoblotting, two bands with electrophoretic mobilities of 51 and 54 kDa were detected by the use of an anti-AZ-1 antibody (Fig. 6*A*) and an anti-FLAG antibody (Fig. 6*B*). Cell extracts from a clone obtained with a control vector gave no significant band in either case. We also prepared immunoprecipitates from the cultured medium of the transfected cells by using anti-AZ-1 antibody. As shown in Fig. 6*C*, immunoblotting of the precipi-

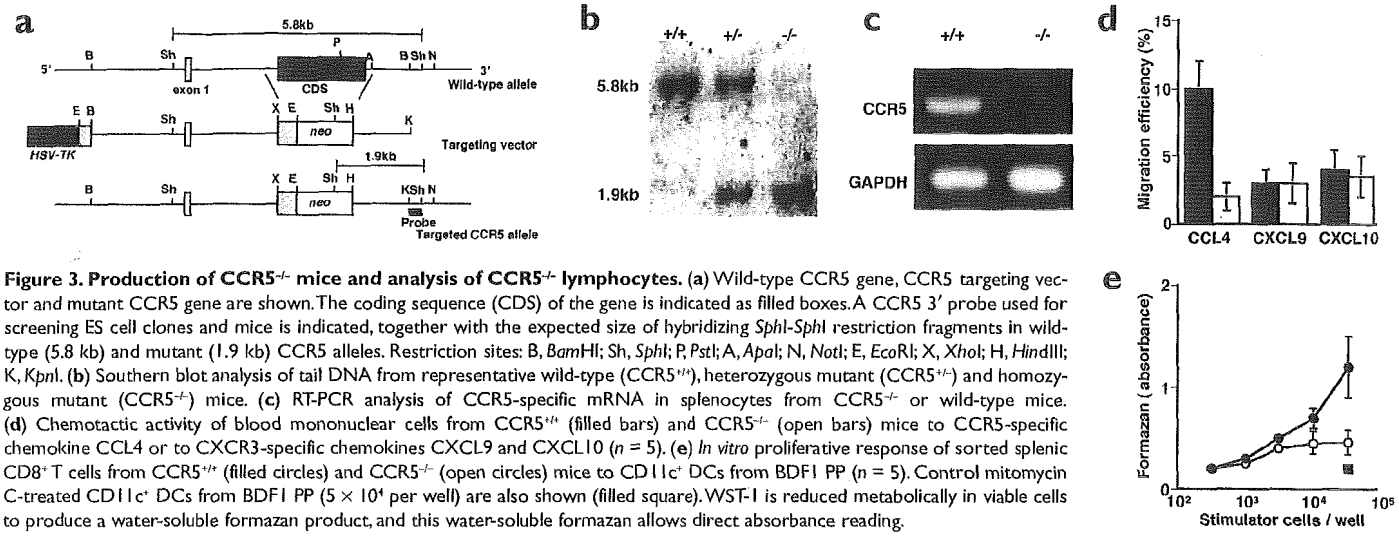

Figure 3. Production of CCR5$^{-/-}$ mice and analysis of CCR5$^{-/-}$ lymphocytes. (**a**) Wild-type CCR5 gene, CCR5 targeting vector and mutant CCR5 gene are shown. The coding sequence (CDS) of the gene is indicated as filled boxes. A CCR5 3′ probe used for screening ES cell clones and mice is indicated, together with the expected size of hybridizing *Sph*I-*Sph*I restriction fragments in wild-type (5.8 kb) and mutant (1.9 kb) CCR5 alleles. Restriction sites: B, *Bam*HI; Sh, *Sph*I; P, *Pst*I; A, *Apa*I; N, *Not*I; E, *Eco*RI; X, *Xho*I; H, *Hin*dIII; K, *Kpn*I. (**b**) Southern blot analysis of tail DNA from representative wild-type (CCR5$^{+/+}$), heterozygous mutant (CCR5$^{+/-}$) and homozygous mutant (CCR5$^{-/-}$) mice. (**c**) RT-PCR analysis of CCR5-specific mRNA in splenocytes from CCR5$^{-/-}$ or wild-type mice. (**d**) Chemotactic activity of blood mononuclear cells from CCR5$^{+/+}$ (filled bars) and CCR5$^{-/-}$ (open bars) mice to CCR5-specific chemokine CCL4 or to CXCR3-specific chemokines CXCL9 and CXCL10 (n = 5). (**e**) *In vitro* proliferative response of sorted splenic CD8$^+$ T cells from CCR5$^{+/+}$ (filled circles) and CCR5$^{-/-}$ (open circles) mice to CD11c$^+$ DCs from BDF1 PP (n = 5). Control mitomycin C-treated CD11c$^+$ DCs from BDF1 PP (5 × 10^4 per well) are also shown (filled square). WST-1 is reduced metabolically in viable cells to produce a water-soluble formazan product, and this water-soluble formazan allows direct absorbance reading.

CCR5, namely, CCL3 and CCL4, were not detected in the host SED on day 2 (data not shown). Furthermore, CCL5 was undetectable in SED of either untreated or isografted BDF1 hosts (data not shown). These results suggest that donor CCR5$^+$CD8$^+$ T cells were attracted to host SED by CCL5 protein that was produced and secreted by host CD11c$^+$ DC, and that CCL5 expression was triggered most likely by initiation of the GVHR in the gut microenvironment.

To further characterize donor CCR5$^+$CD8$^+$ T cells that were attracted to host SED on day 2, we first examined whether donor CD8$^+$ T cells were activated *in situ* or not. This was estimated by measuring the increase in the percentage of replicating cells in donor cells. BrdU was administered to BDF1 hosts intravenously to visualize donor eGFP$^+$ B6 cells that had replicated. Flow cytometric analysis of donor cells showed that there was activation of eGFP$^+$ cells sorted from PP cells, but not spleen and MLN cells (**Fig. 2c**). We then tested whether they exhibit CTL activity against alloantigens of BDF1 hosts. Donor eGFP$^+$CD8$^+$ B6 T cells sorted from PP cells displayed anti-host H-2^d, but not anti-third party H-2^k CTL activities, whereas donor eGFP$^+$CD8$^+$ B6 T cells sorted from spleen cells displayed only marginal anti-host H-2^d CTL activity at this early post-injection period (**Fig. 2d**).

CCR5 and $\alpha_4\beta_7$ involved in induction of a-GVHR

The data presented above indicated that CCR5–CCL5 interactions might be involved in the infiltration of donor CD8$^+$ T cells into host SEDs and

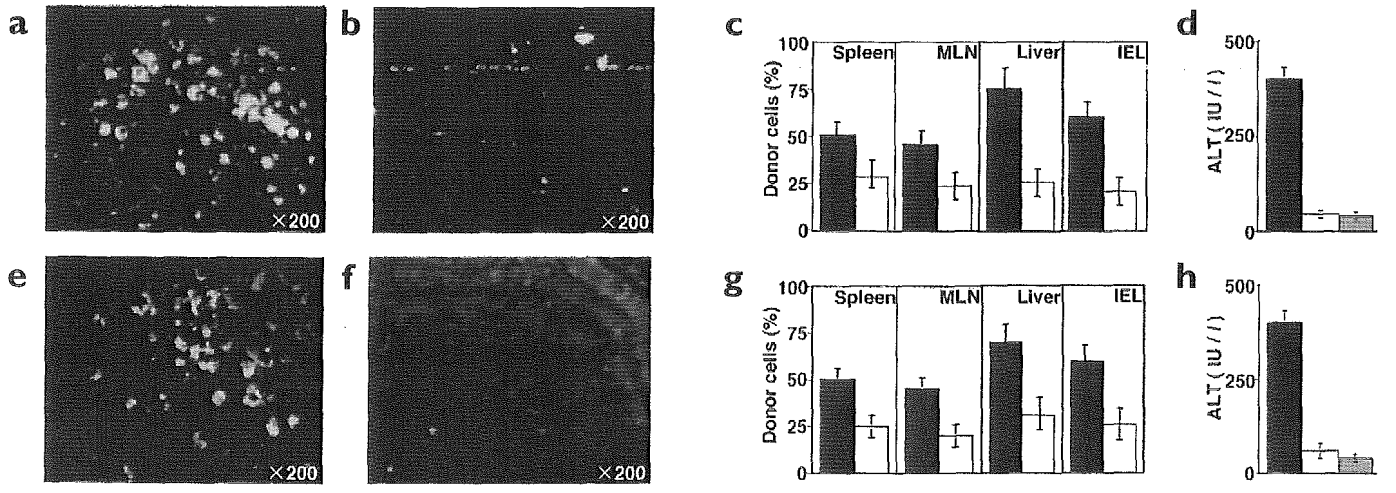

Figure 4. CCR5–CCL5 and $\alpha_4\beta_7$–MAdCAM-1 interactions are implicated in the induction of a-GVHR. We determined the effect of CCR5 gene mutation of donor eGFP$^+$ B6 spleen cells on their ability to infiltrate into various anatomical sites of BDF1 hosts. (**a**) Fluorescence visualization of wild-type (CCR5$^{+/+}$) eGFP$^+$ B6 spleen cells at SED regions of host PPs on day 2 after injection. (**b**) Fluorescence visualization of mutant (CCR5$^{-/-}$) eGFP$^+$ B6 spleen cells at SED region of host PPs on day 2 after injection. (**c**) Population size (%) of wild-type (CCR5$^{+/+}$) (filled bars) and mutant (CCR5$^{-/-}$) (open bars) eGFP$^+$ B6 spleen cells recovered from spleen, MLN, liver and IEL compartments of BDF1 hosts on day 14 after injection (n = 5). (**d**) On day 14 after injection, serum ALT concentration, which is an indicator of liver cell damage, was determined in BDF1 hosts that received wild-type (CCR5$^{+/+}$) eGFP$^+$ B6 spleen cells (filled bar), mutant (CCR5$^{-/-}$) eGFP$^+$ B6 spleen cells (open bar) or syngeneic (CCR5$^{+/+}$) eGFP$^+$ BDF1 spleen cells (shaded bar) (n = 5). We also determined the effect of MAdCAM-1 mAb administration into BDF1 mice on the ability of donor eGFP$^+$ B6 spleen cells to infiltrate into various anatomical sites of BDF1 hosts. (**e**) Fluorescence visualization of eGFP$^+$ B6 spleen cells at SED regions of normal BDF1 host PPs on day 2 after injection. (**f**) Fluorescence visualization of eGFP$^+$ B6 spleen cells at SED regions of mAb-treated BDF1 host PPs on day 2 after injection. (**g**) Population size (%) of donor eGFP$^+$ B6 spleen cells recovered from spleen, MLN, liver and IEL compartments of normal (filled bars) and mAb-treated (open bars) BDF1 hosts on day 14 after injection (n = 4). (**h**) On day 14 after injection, serum ALT concentration, which is an indicator of liver cell damage, was determined in normal (filled bar) and mAb-treated (open bars) BDF1 hosts that received eGFP$^+$ B6 spleen cells (n = 4). The serum concentration of ALT in normal BDF1 hosts that received syngeneic eGFP$^+$ BDF1 spleen cells 14 days in advance (shaded bar) is also shown (n = 4).

© 2003 Nature Publishing Group http://www.nature.com/natureimmunology

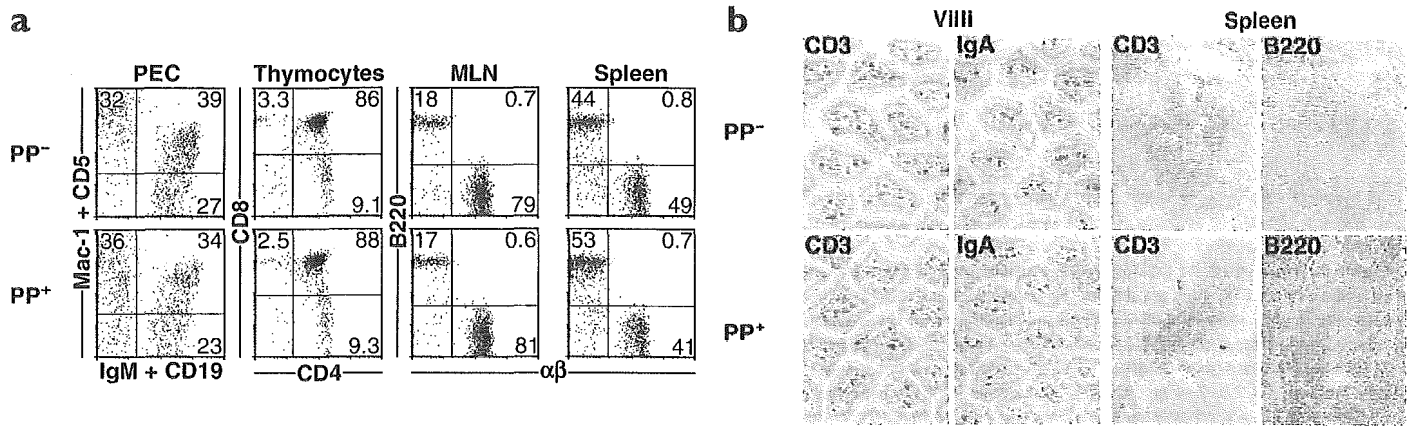

Figure 5. Flow cytometric and immunohistochemical analyses of lymphocytes that reside in BDF1 mice with and without PPs. (**a**) Two-color flow cytometric analysis of lymphocytes isolated from PEC, MLN, spleen and thymus compartments of normal (PP^+) and PP-deficient (PP^-) BDF1 mice. Pictures show the compositions of $IgM^+CD19^+Mac\text{-}1^+CD5^+$ (B-1) and $IgM^+CD19^+Mac\text{-}1^-CD5^-$ (B-2) B cells in the PEC, $CD8^+$ and $CD4^+$ T cells in the thymus, and $B220^+$ B and $TCR\alpha\beta^+$ T cells in the MLNs and spleen. (**b**) Immunohistochemical staining of lymphocytes that settle in the small intestinal villous (original magnification, ×200) and splenic (original magnification, ×60) compartments of normal (PP^+) and PP-deficient (PP^-) BDF1 mice. Villous sections were stained with anti-CD3 or anti-IgA, and splenic sections were stained with anti-CD3 or anti-B220. Comparable numbers of T and B cells (reddish color) can be found in both villous and splenic sections of normal and PP-deficient BDF1 mice.

subsequent development of a-GVHR. To investigate this hypothesis at the molecular level, we generated CCR5-deficient ($CCR5^{-/-}$) B6 mice by the homologous recombination of exon 2 with the gene *neo* (**Fig. 3a–c**). Chemotactic activity of $CCR5^{-/-}$ blood mononuclear cells toward the exclusively CCR5-specific chemokine CCL4 was attenuated, whereas the same $CCR5^{-/-}$ blood mononuclear cells retained a chemotactic response toward CXCR3 ligands CXCL9 and CXCL10 (**Fig. 3d**). The *in vitro* proliferative response of splenic $CD8^+$ T cells from $CCR5^{-/-}$ B6 mice to $CD11c^+$ DCs from BDF1 PPs was decreased compared with that from $CCR5^{+/+}$ B6 mice (**Fig. 3e**).

With these findings in mind, we assessed whether $eGFP^+CCR5^{-/-}$ B6 spleen cells injected into BDF1 mice could induce a-GVHR. Although considerable colonization of control $eGFP^+CCR5^{+/+}$ B6 cells in SEDs was noted on day 2 (**Fig. 4a**), few if any $eGFP^+CCR5^{-/-}$ B6 cells were detected (**Fig. 4b**). On day 14, the percentage of donor $eGFP^+CCR5^{-/-}$ B6 cells in the spleen, MLN, liver and intestinal intraepithelial lymphocyte (IEL) compartments of BDF1 hosts was smaller than that of donor $eGFP^+CCR5^{+/+}$ B6 cells (**Fig. 4c**). Liver injury was not induced in BDF1 hosts that had received $CCR5^{-/-}$ B6 spleen cells, as evidenced by the serum alanine transferase (ALT) concentration (**Fig. 4d**), an indicator of liver cell damage[24] induced by a-GVHD[16].

Next, we evaluated the role of $\alpha_4\beta_7$–MAdCAM-1 (mucosal vascular addressin) interactions in the induction of a-GVHR, as MAdCAM-1 is expressed by venules in the mucosa-associated lymphoid tissues and can direct the migration of T cells expressing integrin $\alpha_4\beta_7$ into intestinal mucosa[15,25]. In sharp contrast to control BDF1

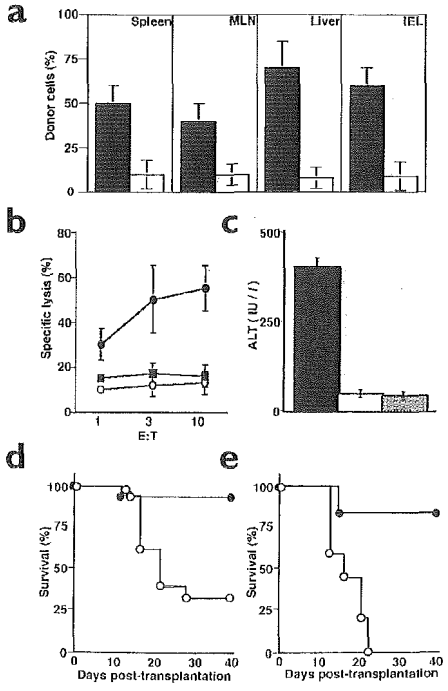

Figure 6. Induction of acute and lethal GVHR is abolished in hosts that lack PPs. (**a–c**) We injected 5×10^7 $eGFP^+$ B6 spleen cells into normal and PP-deficient BDF1 mice. (**a**) Population size (%) of donor $eGFP^+$ cells was determined by flow cytometric analysis of lymphocytes recovered from the spleen, MLN, liver and IEL compartments of normal (filled bars) and PP-deficient (open bars) BDF1 hosts on day 14 after injection ($n = 5$). (**b**) CTL activities of sorted donor $CD8^+$ T cells from spleen of normal BDF1 hosts on day 14 after injection ($n = 5$), anti-host $H\text{-}2^d$ (filled circles) or anti-third party $H\text{-}2^k$ (open circles). CTL activities of sorted donor $CD8^+$ T cells from spleen of PP-deficient BDF1 hosts on day 14 after injection ($n = 5$), anti-host $H\text{-}2^d$ (filled squares). (**c**) On day 14 after injection, serum ALT concentration was determined in normal (filled bar) and PP-deficient (open bar) BDF1 hosts ($n = 6$). Serum ALT concentration of normal BDF1 hosts that received syngeneic $eGFP^+$ BDF1 spleen cells 14 days in advance (shaded bar) is also shown ($n = 6$). (**d**) We injected 8×10^7 B6 spleen cells into 6 Gy-irradiated PP-deficient (filled circles) and normal (open circle) BDF1 mice. Survival of BDF1 hosts was inspected daily. A significantly higher survival rate ($P < 0.05$) was observed in BDF1 mice without PPs ($n = 26$) compared with that observed in BDF1 mice with PPs ($n = 20$). (**e**) Purified $CD8^+$ splenic T cells (1×10^6 cells) from $C.H\text{-}2^{bm1}$ (bm1) mice were injected into 6 Gy-irradiated PP-deficient (filled circles) and normal (open circle) B6 mice. Survival of B6 hosts was prolonged in B6 mice without PPs ($n = 10$) compared with that in B6 mice with PP ($n = 10$).

© 2003 Nature Publishing Group http://www.nature.com/natureimmunology

hosts (**Fig. 4e**), infiltration of donor eGFP$^+$ B6 cells on day 2 into SEDs was virtually abolished in BDF1 hosts that had been pretreated with MAdCAM-1 monoclonal antibody (mAb) (**Fig. 4f**). On day 14 after transfer, the percentage of donor eGFP$^+$ B6 cells in the spleen, MLN, liver and IEL compartments of BDF1 hosts that had received MAdCAM-1 mAb was smaller than that of BDF1 hosts that had received control rat IgG (**Fig. 4g**). Liver injury associated with a-GVHR was not induced in these mAb-treated BDF1 hosts, as serum ALT concentration was not elevated (**Fig. 4h**). These results indicate that both CCR5–CCL5 and $\alpha_4\beta_7$–MAdCAM-1 interactions were required for the infiltration of donor CD8$^+$ T cells into SED and subsequent induction of a-GVHR.

PP-deficient hosts do not develop a-GVHD

To obtain conclusive evidence that the SED of PP is the pivotal anatomical site for the pathogenesis of a-GVHD, we produced PP-deficient BDF1 offspring by administration of IL-7R mAb into B6 pregnant mice[26]. Multiple isolated lymphoid follicles[27], as well as lamina propria lymphocytes, develop normally in the progeny of transplacentally manipulated, PP-deficient B6 mice[27]. Here we corroborated the presence of all well-developed lymphoid organs except PPs in BDF1 offspring from IL-7R mAb-injected B6 mothers. The absolute numbers of lymphocytes (data not shown) and percentages of B cell subsets in the peritoneal cavity (PEC), T and B cells in the MLNs and spleen, and CD4$^+$, CD8$^+$ and CD4$^+$CD8$^+$ T cells in the thymus obtained from BDF1 mice with and without PPs were comparable (**Fig. 5a**). Immunohistochemical analysis revealed that the distribution of CD3$^+$ T and IgA$^+$ B cells in the small intestinal villi and the localization of T and B cells within distinct areas of the spleen were not altered in PP-deficient mice (**Fig. 5b**). We examined whether a-GVHR could be induced in PP-deficient BDF1 mice adoptively transferred with parental B6 splenocytes. On day 14 after injection, absolute numbers of donor eGFP$^+$ B6 cells infiltrating into the secondary lymphoid tissues, such as spleen and MLNs, and target organs, such as liver and intestine, were sharply decreased in PP-deficient mice (**Fig. 6a**). CTL activity against H-2^d alloantigens was not induced in PP-deficient BDF1 hosts (**Fig. 6b**). Likewise, a-GVHD, as indicated by serum ALT release, failed to develop in these mice (**Fig. 6c**).

To address the involvement of PP in host mortality, we further assessed host survival in sublethally (6 Gy) irradiated recipient mice with and without PPs. The survival of BDF1 hosts that had been injected with 8×10^7 B6 spleen cells was prolonged in the absence of PPs (**Fig. 6d**). We used a second model in which a single MHC (major histocompatibility complex) class I mismatched a-GVHR is induced[4,17,28,29] to confirm the involvement of PPs in host mortality. Sublethally irradiated B6 mice with and without PPs were injected with 1×10^6 purified CD8$^+$ splenic T cells from C.H-2^{bm1} (bm1) mice, as the bm1 strain of mice differs from B6 mice only by a single amino acid in the K^b class I molecule[28]. In this donor-host strain combination, a-GVHR is mediated mainly by CD8$^+$ T cells[4,17,28,29]. All ten B6 hosts with PPs died 12 to 21 days after injection, whereas eight of ten B6 hosts without PPs survived until day 40 after injection (**Fig. 6e**).

Discussion

a-GVHD is one of the major obstacles for BMT and reflects the life-threatening outcome of complex cellular events involving multigenic effects[1,2,4–11,18,19]. In this study, we took a closer look at the pathophysiology of a-GVHD by analyzing a well-established mouse a-GVHR model[3,6,11,16–19,28,29]. On day 2 after injection of donor eGFP$^+$ spleen cells into unirradiated BDF1 mice, an equivalent number of donor CD8$^+$ T cells migrated into the host spleen and PPs. However, compared with donor eGFP$^+$ cells collected from host spleen, the cells collected from host PPs displayed a much higher frequency of DNA replicating cells and retained much stronger anti-host CTL activity. Alloantigen-activated donor CBA T cells collected from the thoracic duct of irradiated (CBA × B6)F1 mice (which had been injected in advance with parental CBA T cells) homed selectively, within 24 hours, to the small intestine of syngeneic CBA mice upon transfer[30,31]. They also showed that CBA thymocytes migrated into the spleen and lymph nodes during the first 24–48 hours after adoptive transfer into irradiated (CBA × B6)F1 recipients[32]. In this study[32], however, donor T cell migration into the F1 intestines was not examined. Thus, the previous findings[30,31] and our present findings are not mutually exclusive, and homing to the intestine seems to be a general property of T cells activated to transplantation antigens. Our data also corroborate that both CCR5–CCL5 and $\alpha_4\beta_7$–MAdCAM-1 interactions are indispensable, not only for the influx of donor CD8$^+$ T cells into the SED region of PPs, but also for the consequent induction of a-GVHD. The high risk of host mortality caused by a-GVHR is ameliorated in PP-deficient recipient mice.

Another notable observation relates to the transplacentally manipulated PP-deficient, but otherwise normal, hosts. Consistent with our observations, previous studies showed that the organogenesis and cellular composition of the unaffected primary and secondary lymphoid organs remain intact in the PP-deficient condition[26,27]. Moreover, we confirmed that both humoral and T cell proliferative immune responses to a protein antigen (that is, bovine serum albumin) elicited from mice without PPs are comparable to those elicited from mice with PPs (H.H. and H.I. *et al.*, unpublished observations). Thus, it is now evident that the SED region of gut PPs is the essential locale in initiating this well-characterized murine a-GVHR.

PPs are the major sites of lumenal antigen and microorganism sampling[21–23,33,34], which leads to continuous immune responses. As a consequence of this, lymphocytes that settle in intestinal mucosa are highly active[7,35,36] and produce various cytokines, chemokines and adhesion molecules[7,16,17,34,36]. Among numerous lumenal antigens such as food-derived allergens, commensal microbes constitute the largest antigenic load in the gut lumen[7,34,36–38] and have a critical role in establishing the intestinal immune system[37,38]. In fact, mice kept under "germ-free" conditions have sharply attenuated GALT[37,39] (gut-associated lymphoid tissue), are insusceptible to oral tolerance induction[40], do not develop inflammatory bowel diseases[37,41] and are relatively resistant to lethal GVHD[42]. It has also been demonstrated that endotoxin, or LPS, a component of intestinal flora known as a potent enhancer of inflammatory cytokine release, is involved in the early events contributing to the onset of a-GVHD[43–45]. GVHD has been viewed as a normal reaction of normal donor lymphocytes to what seems, to the immune system, to be a serious infection[7]. Others suggested that GVHD might be particularly severe in an inflammatory context[46]. Overall, our present data, which establish that the PPs of the alimentary tract are the pivotal birthplace of donor-derived, anti-host CTL causing a-GVHD, is in line with the continued elucidation of distinctive features inherent to the gut immune system.

The SED is well positioned for the processing of lumenal antigens passing into PPs from the overlying M cells and harbors a distinct subset of DCs[21–23,47] that are capable of differentiating into two functionally distinct DCs. In view of these recent findings, it is conceivable that the SED is a specialized lymphoid compartment that retains as yet unresolved immunologically relevant competencies, examples of which are the selective and considerable infiltration of donor B6 CD8$^+$ T cells into host BDF1 SEDs and the subsequent *in situ* development of anti-host CTL. In conclusion, it is now evident that PPs, most likely the

© 2003 Nature Publishing Group http://www.nature.com/natureimmunology

SED region of PPs, is the essential lymphoid compartment in initiating well-characterized murine a-GVHR, and the present findings will provide us with ideas to prevent a-GVHD in BMT therapy.

Methods

Mice. C57BL/6 (B6; H-2^b), DBA/2 (H-2^d), C3H/HeN (H-2^k) and (C57BL/6 × DBA/2)F1 (*BDF1*; H-2$^{b \times d}$) *mice were purchased from Charles River (Yokohama, Japan).* C.H-2^{bm1} (bm1) mice were purchased from The Jackson Laboratory (Bar Harbor, ME). B6 mice carrying the eGFP transgene[20] were provided by M. Okabe (Osaka University). To generate BDF1 mice carrying the eGFP transgene, eGFP B6 mice were crossed with DBA/2 mice. We obtained manipulated PP-deficient BDF1 and B6 mice as described[26,27]. In brief, timed-pregnant B6 mothers were injected intravenously with 2 mg of an antagonistic mAb to IL-7R (A7R34)[26,27] on gestational day 14.5. The A7R34 was a gift from S. Nishikawa (Kyoto University). All animal procedures described in this study were performed according to the guidelines for animal experiments of The University of Tokyo.

Generation of CCR5-deficient mice. Genomic DNA containing the CCR5 locus was isolated from the DNA library of the 129 mouse strain (Stratagene, La Jolla, CA). Exon 2 of the CCR5 gene was deleted and replaced with a *neo* gene, and herpes simplex virus thymidine kinase (*HSV-TK*) gene was fused to the 5′ end (**Fig. 3a**). The *neo* gene is flanked by 7-kb and 0.9-kb DNA fragments from the *CCR5* locus. This targeting vector was inserted in E14.1 cells by electroporation, and homologous recombination events were enhanced by selection with G418 and ganciclovir and identified by polymerase chain reaction (PCR) analysis. Two independently mutated ES colonies were used to produce mutant mice by blastocyst injection. Southern blot analysis confirmed the deletion of coding sequence for the CCR5 gene in CCR5 gene-deficient (CCR5$^{-/-}$) mice (**Fig. 3b**), and RT–PCR analysis showed the absence of CCR5-specific mRNA in lymphocytes from CCR5$^{-/-}$ mice (**Fig. 3c**). Primers used for RT-PCR analysis were as follows: forward, 5′-TCCGGAGTTATCTC TCAGTGTTCTTCCG-3′; reverse, 5′-GTCACAGGACTCTGGTTTCACAATCAGA-3′. CCR5$^{-/-}$ 129 mice were backcrossed six times to B6 parent and then crossed with B6 mice carrying the eGFP transgene to obtain eGFP$^+$CCR5$^{-/-}$ and eGFP$^+$CCR5$^{+/+}$ B6 mice. To confirm that the CCR5$^{-/-}$ mice were functionally null for CCR5, we analyzed the chemotactic activity of blood mononuclear cells using a 96-well chemotaxis chamber (Neuroprobe, Pleasanton, CA) with polycarbonate filter (3-μm pore size). The migration efficiency was measured as the percentage of input cells that had migrated into the lower chambers containing the optimal concentration (100 ng/ml) of CCL4, CXCL9 or CXCL10 (R&D Systems, Minneapolis, MN; **Fig. 3d**).

Induction of GVHR. In most of our experiments, 5 × 10^7 spleen cells from parental eGFP$^+$ B6 mice were injected intravenously into unirradiated BDF1 mice. To determine host mortality, sublethally (6 Gy)-irradiated BDF1 mice with and without PP were injected with 8 × 10^7 spleen cells from parental B6 instead of eGFP$^+$ B6 mice. We also injected 1 × 10^6 purified CD8$^+$ splenic T cells from bm1 mice into 6 Gy-irradiated B6 mice with and without PP. CD8$^+$ splenic T cells were enriched by isolation of CD8-positive cells with the magnetic-activated cell sorting system (MACS; Miltenyi Biotec, Auburn, CA).

Inspection and modulation by MAdCAM-1 mAb of GVHR. GVHR induced in unirradiated BDF1 hosts was assessed by the number and the population size of donor eGFP$^+$ cells that had been colonized in PP, spleen, MLN, liver and IEL compartments of BDF1 hosts on day 2 and day 14 after donor cell injection. Liver damage was assessed on day 14 after donor cell injection by serum ALT concentrations[24] as an indication of a-GVHD. MAdCAM-1 mAb (MECA-367; BD PharMingen, San Diego, CA) was administered (100 μg per mouse) intravenously into BDF1 mice shortly before the injection of donor B6 spleen cells to assess the effect of interfering MAdCAM-1 function on the induction of a-GVHR.

Immunofluorescence staining. For immunofluorescence analysis of PPs, the intestinal tissue fragments that contain PPs were fixed in paraformaldehyde, washed with PBS, embedded in Tissue-Teck OCT compound (Miles, Elkhart, IN) at –80 °C and sectioned with a cryostat at 6 μm, and sections were preincubated with Fc Block (BD PharMingen), which contained 10% normal mouse serum (Sigma, St. Louis, MO), for 30 min at room temperature to block nonspecific binding of mAbs. The sections were then incubated with the following mAbs obtained from BD PharMingen; phycoerythrin (PE)-conjugated rat anti-CD8α (Ly-2; 5 μg/ml), anti-CD4 (L3T4; 1 μg/ml), anti-CCR5 (C34-3448; 10 μg/ml), anti-$\alpha_4\beta_7$ (DATK32; 5 μg/ml) or anti-CD11c (HL-3; 5 μg/ml). For detection of CD11c and CCL5 expression, 5 × 10^7 spleen cells obtained from parental B6 instead of eGFP$^+$ B6 mice were injected into BDF1 hosts, and the intestinal tissue sections containing PP that had been incubated with fluorescein (FITC)-conjugated CD11c mAb (PharMingen) and biotinylated polyclonal goat CCL5 IgG Abs (R&D Systems) were incubated with Texas red-conjugated streptavidin (Jackson ImmunoResearch, West Grove, PA). Finally, the sections were analyzed by an Olympus AX-80 fluorescence microscope (Olympus Optical Co., Ltd., Tokyo, Japan).

Immunohistochemistry. The following mAbs from BD PharMingen were used: hamster anti-mouse CD3 (145-2C11; 5 μg/ml), rat anti-mouse IgA (C10-3; 0.5 μg/ml) and rat anti-mouse B220 (RA3-6B2; 2 μg/ml). The tissue segments were sectioned with a cryostat at 6 μm and sections were preincubated with Block-ace (Dainippon Pharmaceutical Co., Ltd., Osaka, Japan) to block nonspecific binding. The sections were then incubated with rat or hamster mAb for 30 min at 37 °C, and rinsed three times with PBS, followed by incubation with biotin-conjugated goat anti-rat IgG (5 μg/ml, Cedarlane Laboratories Limited, Ontario, Canada) or with biotin-conjugated goat anti-hamster IgG (5 μg/ml, Cedarlane Laboratories Limited). Subsequently, the sections were washed three times with PBS and then incubated with avidin–biotin peroxidase complexes (Vectastain ABC kit, Vector Laboratories, Inc., Burlingame, CA). The histochemical color development was achieved by Vectastain DAB (3,3′-diaminobenzidine) substrate kit (Vector Laboratories, Inc.) according to the manufacturer's instructions. Finally, the sections were counter-stained with hematoxylin for microscopy. Endogenous peroxidase activity was blocked with 0.3% H_2O_2 and 0.1% NaN_3 in distilled water for 10 min at room temperature. Tissue sections incubated either with isotype-matched normal rat IgG or with non-immune hamster serum showed only minimal background staining.

Flow cytometry. The following mAbs from BD PharMingen were used: FITC-conjugated anti-IgM (II/4-1; 20 μg/ml), anti-CD19 (1D3; 5 μg/ml), anti-TCRαβ (H57-597; 5 μg/ml) and anti-CD4 (GK1.5; 5 μg/ml); and biotinylated anti-Mac-1 (M1/70; 5 μg/ml), anti-CD5 (53-7.3; 2.5 μg/ml), anti-B220 (RA3-6B2; 2.5 μg/ml) and anti-CD8α (53-6.7; 25 μg/ml). A single lymphoid cell suspension was prepared and nucleated cells were counted using a hemocytometer. Resident lymphoid cells in the PEC were obtained by rinsing PEC with 10 ml of ice-cold PBS without Ca^{++} and Mg^{++}. Lymphoid cells were incubated first with biotinylated mAb and then with streptavidin-PE (Becton Dickinson) and FITC-conjugated second mAb. Stained cells were suspended in staining medium (Hanks' solution without phenol red, 0.02% NaN_3 and 2% heat-inactivated fetal bovine serum) containing 0.5 μg/ml propidium iodide (PI) and analyzed using FACScan with CELLQuest software (Becton Dickinson). Dead cells were excluded by PI gating. Lymphoid cells were incubated with anti-FcγR II/III mAb (2.4G2, 10 μg/ml; PharMingen) before staining to block nonspecific binding of labeled mAbs to FcR.

***In vivo* labeling and flow cytometric analysis of DNA replicating cells.** One hour after the single intravenous infusion of 0.5 mg 5-bromo-2′-deoxyuridine (BrdU; Sigma) into BDF1 hosts that had been injected 2 days before with parental eGFP$^+$ B6 spleen cells, lymphoid cell suspensions were prepared from PP, spleen and MLN, and donor-derived eGFP$^+$ cells were sorted with an EPICS Elite cell sorter (Coulter Electronics Ltd., Hialeah, FL). Purified eGFP$^+$ cells were incubated with biotinylated anti-BrdU according to the manufacturer's instructions (Zymed Laboratories, San Francisco, CA), followed by incubation with streptavidin-Alexa fluor 594 (Molecular Probes, Eugene, OR). Stained cells were analyzed by EPICS Elite flow cytometry (Coulter Electronics Ltd.).

Cytotoxicity assay. PP and spleen cells were isolated from BDF1 hosts that had been injected with parental eGFP$^+$ B6 spleen cells, and CD8$^+$ T cells were enriched as described previously. Subsequently, donor-derived CD8$^+$ T cells expressing eGFP molecules were sorted with an EPICS Elite cell sorter (Coulter Electronics Ltd.). Sorted effector (E) eGFP$^+$CD8$^+$ B6 (H-2^b) T cells were incubated with 5 × 10^3 target (T) spleen cells from DBA/2 (H-2^d) or C3H/HeN (H-2^k) mice for 10 h at 37 °C in 200 μl culture medium (RPMI 1640 medium containing 1% FCS/4 mM glutamine/penicillin at 100 units/ml streptomycin at 100 μg/ml) in each well of round-bottom, 96-well microtiter plates (Nunc, Copenhagen, Denmark). After the incubation, cytotoxicity was determined by measuring the quantity of lactate dehydrogenase (LDH) released into supernatant[48] using a LDH cytotoxicity detection kit (Takara Biomedicals, Tokyo, Japan). All determinations were carried out in triplicate using three E:T ratios. The percent specific LDH release was calculated from: (experimental release – spontaneous release) / (detergent-induced release – spontaneous release) × 100.

Mixed lymphocyte and DC culture. The one-way mixed leukocyte reaction was performed in each well of round-bottom, 96-well microtiter plates (Nunc) using the Premix WST-1 cell proliferation assay system (Takara Biomedicals) according to the manufacturer's instructions[49]. PP-derived DCs were prepared from BDF1 mice according to described methods[49], with slight modifications. In brief, PP were digested with collagenase D and incubated in the presence of 5 mM EDTA at 37 °C for 5 min. The cell suspensions prepared were incubated with anti-CD11c coated magnetic beads (Miltenyi Biotec). Sorted PP-derived CD11c$^+$ DCs were treated with 20 μg/ml mitomycin C at 37 °C for 30 min and washed three times with PBS. CD8$^+$ T cell-enriched spleen cells (4 × 10^5) from either eGFP$^+$CCR5$^{-/-}$, eGFP$^+$CCR5$^{+/+}$ or BDF1 (negative control) mice were cultured in triplicate with various numbers of mitomycin C–treated DCs from BDF1 PPs for 72 h at 37 °C in 200 μl complete culture medium (RPMI 1640 medium containing 10% FCS/4 mM glutamine/penicillin at 100 units/ml streptomycin at 100 μg/ml) in each well of round-bottom 96-well microtiter plates (Nunc). Four hours before the end of culture, WST-1 (water-soluble tetrazolium salt; 4-[3-(4-iodophenyl)-2-(4-nitrophenyl)-2H-5-tetrazolio]-1,3-benzene disulfonate sodium salt) (20 μl) was added and the absorbance (450–650 nm) was measured[49].

Biochemical analysis. The increase in serum ALT concentration, which is an indicator of liver cell damage[24], was determined with a Fuji DRY-CHEM 5500V (Fuji Medical Systems, Tokyo, Japan) according to the manufacturer's instructions.

Note: Supplementary information is available on the Nature Immunology *website.*

Acknowledgments

We thank J.J. Oppenheim, K. Matsuno, S. Ishikawa, M. Haino and C.Vestergaard for helpful discussions and S. Fujita for assistance in animal surgery. This work was supported by

© 2003 Nature Publishing Group http://www.nature.com/natureimmunology

tates using anti-FLAG antibody showed 51- and 54-kDa polypeptides. A faint 52-kDa band seen with the medium of the control clone (Fig. 6*C*, *lane 5*) was likely to result from a cross-reactivity of the secondary antibody to the heavy chain of bovine or horse IgG in the culture medium. These results were consistent with the presence of the signal peptide sequence at the N terminus of the deduced amino acid sequence of AZ-1.

The difference in the molecular mass of the AZ-1F protein detected with transfected cells (54 and 51 kDa) from that of the *in vitro* synthesized polypeptide (47 kDa) may be attributable to post-translational modification. To examine *N*-glycosylation of the polypeptide produced in the transfected cells, the cells were incubated with tunicamycin, and the cell extracts were analyzed by immunoblotting with anti-AZ-1 antibody. As shown in Fig. 6*D*, a 48-kDa band was detected after the tunicamycin treatment in addition to the 54- and 51-kDa bands, and *N*-glycanase treatment of the cell extracts from the transfected cells also produced a 48-kDa band (Fig. 6*E*). These results suggested that AZ-1 protein was post-translationally *N*-glycosylated in the cells.

Inverse Correlation between AZ-1 and Cyp11b-1 Expression in Clonal Lines Derived from Y-1 Cells—The expression levels of AZ-1 mRNA in the cell lines used for the subtractive cloning were apparently in an inverse correlation to the levels of Cyp11b-1 mRNA (25). The effects of expression of the AZ-1 protein on the phenotypes of Y-1 cells then were examined by analyzing mRNA levels of the steroidogenic genes in the transfectants (Fig. 7). We analyzed 10 clones of mock transfectants obtained with a control DNA and 11 clones obtained with an AZ-1F expression vector. Fig. 7*A* shows that mRNA encoding AZ-1F was detected in 4 clones (*lanes 12, 13, 15,* and *18*) among the 11 clones isolated after transfection with the AZ-1F expression vector, whereas no AZ-1F mRNA was detectable among the 10 clones transfected with the control vector (*lanes 1–10*). A PCR primer pair that was able to detect mRNA of both the endogenous *Az-1* gene and AZ-1F was used. Unexpectedly, 7 of 10 control clones were found to express significant levels of the endogenous *Az-1* gene mRNA (Fig. 7*B*, *left*). Among the 11 clones obtained with transfection of the AZ-1F vector, 6 clones (*lanes 12, 13, 15, 18, 20,* and *21*) expressed mRNA of either the endogenous or exogenous *Az-1* genes, indicating that the endogenous *Az-1* gene was expressed in at least two clones (*lanes 20* and *21*). The reason for the induction of the endogenous *Az-1* gene through the selection procedure for the transfectants was unknown. Fig. 7*C* shows that Cyp11b-1 mRNA was undetectable only in the clones expressing either AZ-1 from the endogenous gene or AZ-1F. On the other hand, Cyp11a mRNA was detectable in all of the 21 clones with various levels (Fig. 7*D*). The experiments with a GAPDH primer pair monitored efficiencies of reverse transcription and amplification from the RNA preparations (Fig. 7*E*). Fig. 7*F* depicts the inverse correlation of the mRNA levels between AZ-1 and Cyp11b-1 (*closed circles*); the clones expressing a very low or undetectable level of the endogenous *Az-1* gene mRNA expressed Cyp11b-1 mRNA, whereas those expressing higher levels of the AZ-1 mRNA did not express Cyp11b-1 mRNA. The same correlation was observed for the 4 lines expressing AZ-1F (*closed triangles*). On the other hand, Cyp11a mRNA was expressed irrespective of AZ-1 expression (*open circles* and *open triangles*). These results indicated that Cyp11b-1 was expressed in the clonal lines maintaining little AZ-1 expression and became undetectable in those expressing AZ-1.

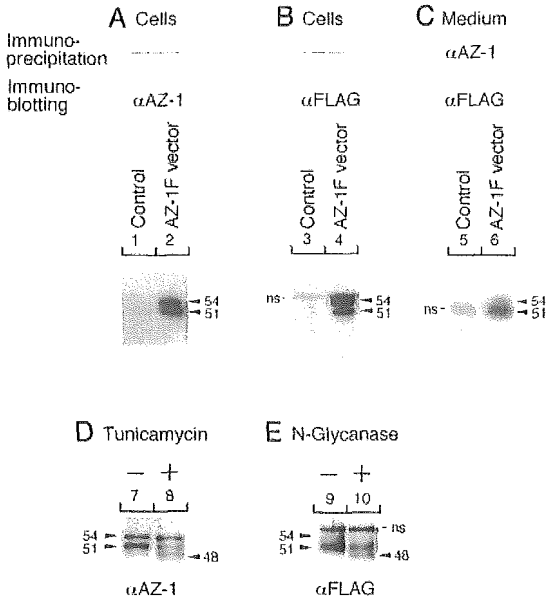

FIG. 6. **Detection of AZ-1 protein produced in stable transfectants and *N*-glycosylation.** *A–C*, Y-1 cells stably transfected with a *control* vector pRc/CMV (*lanes 1, 3,* and *5*) or with an expression vector pR/C11.13FD1 encoding FLAG epitope-tagged AZ-1 (*AZ-1F, lanes 2, 4,* and *6*) were cultured for 24 h at 37 °C. Whole cell extracts were analyzed by immunoblotting using chicken anti-AZ-1 antibody (*lanes 1* and *2*) and anti-FLAG antibody (*lanes 3* and *4*). Immunoprecipitates (*lanes 5* and *6*) from the culture media of the transfectants with chicken anti-AZ-1 antibody were analyzed by immunoblotting using anti-FLAG antibody as described under "Experimental Procedures." *D*, the AZ-1F-expressing cells were cultured in the presence of vehicle (*lane 7*) or 10 μg/ml tunicamycin (*lane 8*) for 18 h. Whole cell extracts were analyzed by immunoblotting with anti-AZ-1 antibody. *E*, whole cell extracts of the AZ-1F-expressing cells were incubated in the absence (*lane 9*) or presence (*lane 10*) of 50 units/ml *N*-glycosidase F (*N-glycanase*) at 37 °C for 18 h. They were analyzed by immunoblotting with anti-FLAG antibody. *ns*, nonspecific signals.

DISCUSSION

AZ-1 cloned in the present study turned out to be a putative factor involved in the zonal differentiation of adrenocortical cells, as judged by the solid inverse correlation between expression of AZ-1 and Cyp11b-1 both *in vitro* and *in vivo*. Although it has not been established if AZ-1 plays a causal role as a direct signal in repressing the *Cyp11b-1* gene, the current results led us to conclude that expression of AZ-1 is coupled with mechanisms determining the functional differentiation of the cortex. As compared with known factors that determine differentiation of adrenocortical cells, AZ-1 showed distinct features. First, AZ-1 is an extracellular protein with unique EGF domains and a catalytically inactive proteinase domain related to cathepsin B. Second, different from SF-1 that is essential for development of the tissue and occurs throughout the adrenocortical zones (19, 20), AZ-1 is expressed in a spatially restricted manner and is implicated in the adrenocortical zonation. Third, in contrast to AP-1 which we have previously identified as an activator for the *Cyp11b-1* gene expression (23, 24), AZ-1 is apparently involved in mechanisms for repressing the gene. Topographic distribution of AP-1 *in vivo* also agrees well with the function of selectively activating the *Cyp11b-1* gene expression (23, 24). Collectively with our previous studies, the present results suggest that AP-1 and AZ-1 are expressed in a mutually exclusive manner that topographically corresponds to the actual functions of the cells to execute the zone-specific steroidogenesis.

Recent studies from other investigators have suggested the presence of factors occurring in a zone-specific manner that could simultaneously regulate the zonal differences in the adrenocortical steroidogenesis. Preadipocyte factor 1 (40) (also called zona glomerulosa-specific protein) was reported as such a candidate that is expressed in cells of zG of rats (41). Based on an inhibitory function of preadipocyte factor 1/zona glo-

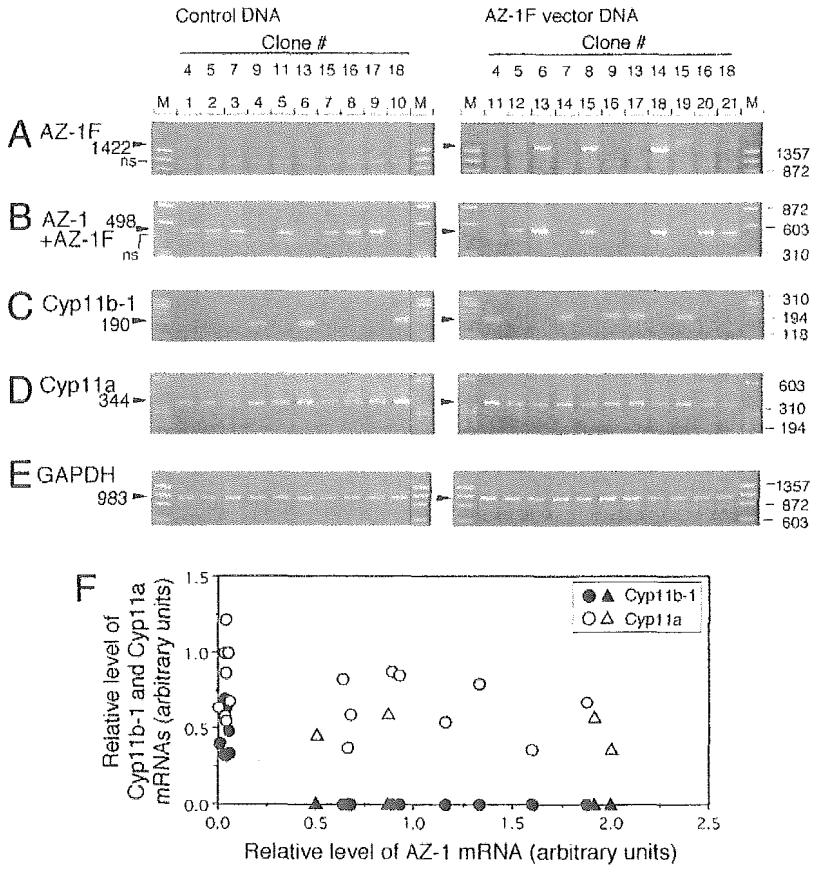

FIG. 7. **Inverse correlation between AZ-1 and Cyp11b-1 expression in clonal lines derived from Y-1 cells.** RNAs from 10 stable transfectants obtained with pRc/CMV (*control DNA*) and 11 obtained with pR/C11.13FD1 (*AZ-1F vector DNA*) were analyzed by RT-PCR. cDNAs synthesized with oligo(dT) primer using total RNA (1 μg) were amplified by PCR using specific primer pairs for FLAG-tagged AZ-1 (*AZ-1F*) (*A*), both the endogenous AZ-1 and AZ-1F (*B*), steroid 11β-hydroxylase (*Cyp11b-1*) (*C*), cholesterol side-chain cleavage enzyme (*Cyp11a*) (*D*), and glyceraldehyde-3-phosphate dehydrogenase (*GAPDH*) (*E*) as described under "Experimental Procedures." PCR products (15 μl) were analyzed through 2% agarose gels and visualized with ethidium bromide. *Numbers* with *arrowheads* indicate sizes of the products. *ns*, nonspecific band. Amplified conditions were within the exponential phase of the reactions to obtain the linear dose response concerning the initial mRNA amounts. *F*, relationships of normalized mRNA levels between AZ-1 and Cyp11b-1 and between AZ-1 and Cyp11a. For the 17 clonal lines without expression of AZ-1F, relationships of mRNA levels of Cyp11b-1 (*closed circle*) or Cyp11a (*open circle*) to those of the endogenous *Az-1* gene are shown. For the other four lines (clones 5, 6, 8, and 14; AZ-1F-expressing lines), the relationships of the mRNA levels of Cyp11b-1 (*closed triangle*) or Cyp11a (*open triangle*) to those of the endogenous *Az-1* gene plus AZ-1F are shown.

merulosa-specific protein in the differentiation of preadipocytes (40) together with its expression patterns through the development of the adrenal cortex, this factor is presumed to have a role in the functional differentiation of the adrenocortical zones (42). Inner zone antigen is another candidate occurring in zFR in rat adrenal cortex that was identified to be a putative membrane progesterone receptor (43). Because anti-inner zone antigen antibody inhibited activities of Cyp11b-1 in addition to steroid 21-hydroxylase *in vitro* (44), the factor seemed to be implicated in the steroidogenesis of zFR. For identification of these factors, functionally differentiated cells *in vivo* such as cells of zG and zFR of rats were utilized as the resource materials. Although such methodologies used in these previous studies turned out to be useful in obtaining the specific molecular markers for the adrenocortical zones (41, 45), their functions in the zone-specific steroidogenesis and/or in the development of the zones still remain to be elucidated. In order to overcome difficulties to search for factor(s) involved in the functional differentiation, we herein used the recently established adrenocortical cell line AcA101 at an undifferentiated state as the alternative resource material. In this context, the present study employing a different strategy has revealed that the novel factor whose expression was accompanied by the lack of expression of Cyp11b-1 was responsible for the zone-specific steroidogenesis. Thus, regulation of the *Az-1* gene is interconnected with determining the zonal structures of the adrenal cortex.

At the same time, the current results raise further questions as to the function of AZ-1 in the zonal differentiation of adrenocortical cells. Because expression of the endogenous *Az-1* gene was induced through the selection processes for stably transfected cells, direct evidence that cells expressing AZ-1 are devoid of Cyp11b-1 expression was obtained. Although AZ-1 was shown to be secreted in the culture medium by using the transfected cells, it is unknown at present whether the secreted form of AZ-1 could repress expression of the *Cyp11b-1* gene by a signaling through the cell surface. Another important issue for the adrenocortical zonation is identification of molecules that determine expression of Cyp11b-2 in cells of zG. Based on the present findings that Cyp11b-2 is expressed in the AZ-1-positive cells *in vivo* and that the Cyp11b-1 is expressed in AZ-1-negative cells *in vivo*, we speculate that AZ-1 is a prerequisite for cells of zG to express Cyp11b-2 without expression of Cyp11b-1. Identification of such factors occurring in cells of zG that determine Cyp11b-2 expression deserves further studies provided that a combination of AZ-1 with them could actually determine the functional differentiation of cells in zG.

The primary structure of AZ-1 protein suggests that it carries the potential to play a role in formation of the cell arrangements in the adrenal cortex. Among the novel protein family to

which AZ-1 belongs, functions of TIN-ag have well been characterized (37, 46). TIN-ag has been shown to be essential for development of glomeruli in embryonic kidney (37), suggesting that TIN-ag is involved in the epithelial-mesenchymal interactions. Furthermore, despite the replacement of the cysteine residue essential for the proteolytic activity of cathepsin B (47–49), it was shown that purified TIN-ag binds to laminin and type IV collagen and inhibits polymerization of laminin (46). Because AZ-1 shares essentially the same structural features as TIN-ag, AZ-1 could interact with extracellular matrix proteins. These molecules are generally involved in arrangements of cells in multicellular systems including tumor invasion. It may not be unreasonable to postulate that AZ-1 functions to regulate the arrangement of adrenocortical cells through such cell-to-cell and/or cell-to-matrix interactions.

Previous studies using chimeric (50) and transgenic (51) animals have suggested that adrenocortical cells arranging centripetally are clonal cells; a progenitor cell differentiates into two functionally distinct cell species, cells of zG and those of zFR. Thus, two patterns of the cell arrangement are likely to be present in the adrenal cortex: the centripetal arrangements of clonal cells and the concentric arrangements of functionally differentiated cells. By analogy with the structure of TIN-ag, it can be hypothesized that AZ-1 plays a role in development and maintenance of the cell arrangements. Further characterization of such an effect of AZ-1 on the cell arrangements through the interaction with matrix proteins and its functional link to steroidogenic gene regulation is now underway in this laboratory.

Acknowledgments—We thank M. Kondo and K. Kondo for preparation of adrenal sections and Y. Nagatsuka for assistance in affinity purification of the antibodies.

REFERENCES

1. Orth, D. N., Kovacs, W. J., and DeBold, C. R. (1992) in *Williams Textbook of Endocrinology* (Wilson, J. D., and Foster, D. W., eds) pp. 489–619, W. B. Saunders Co., Philadelphia
2. Cain, A. J., and Harrison, R. G. (1950) *J. Anat.* **84,** 196–226
3. Cater, D. B., and Lever, J. D. (1954) *J. Anat.* **88,** 437–454
4. Deane, H. W., and Greep, R. O. (1946) *Am. J. Anat.* **79,** 117–145
5. Hall, K., and Korenchevsky, V. (1937) *Nature* **140,** 318–318
6. Hartroft, P. M., and Eisenstein, A. B. (1957) *Endocrinology* **60,** 641–651
7. Mitchell, R. M. (1948) *Anat. Rec.* **101,** 161–185
8. Nicander, L. (1952) *Acta Anat.* **14,** (suppl.) 16
9. Reiss, M., Balint, J., Oestreicher, F., and Aronson, V. (1936–7) *Endokrinologie* **18,** 1–10
10. Mitani, F., Suzuki, H., Hata, J., Ogishima, T., Shimada, H., and Ishimura, Y. (1994) *Endocrinology* **135,** 431–438
11. Ogishima, T., Mitani, F., and Ishimura, Y. (1989) *J. Biol. Chem.* **264,** 10935–10938
12. Mitani, F., Mukai, K., Miyamoto, H., Suematsu, M., and Ishimura, Y. (2003) *Biochim. Biophys. Acta,* **1619,** 317–324
13. Mitani, F., Ogishima, T., Miyamoto, H., and Ishimura, Y. (1995) *Endocr. Res.* **21,** 413–423
14. Mitani, F., Miyamoto, H., Mukai, K., and Ishimura, Y. (1996) *Endocr. Res.* **22,** 421–431
15. Mitani, F., Mukai, K., Ogawa, T., Miyamoto, H., and Ishimura, Y. (1997) *Steroids* **62,** 57–61
16. Mitani, F., Mukai, K., Miyamoto, H., and Ishimura, Y. (1998) *Endocr. Res.* **24,** 983–986
17. Mitani, F., Mukai, K., Miyamoto, H., Suematsu, M., and Ishimura, Y. (1999) *Endocrinology* **140,** 3342–3353
18. Miyamoto, H., Mitani, F., Mukai, K., Suematsu, M., and Ishimura, Y. (2000) *Endocr. Res.* **26,** 899–904
19. Parker, K. L., and Schimmer, B. P. (1997) *Endocr. Rev.* **18,** 361–377
20. Morohashi, K. I., and Omura, T. (1996) *FASEB J.* **10,** 1569–1577
21. Luo, X., Ikeda, Y., and Parker, K. L. (1994) *Cell* **77,** 481–490
22. Morohashi, K., Iida, H., Nomura, M., Hatano, O., Honda, S., Tsukiyama, T., Niwa, O., Hara, T., Takakusu, A., Shibata, Y., and Omura, T. (1994) *Mol. Endocrinol.* **8,** 643–653
23. Mukai, K., Mitani, F., Shimada, H., and Ishimura, Y. (1995) *Mol. Cell. Biol.* **15,** 6003–6012
24. Mukai, K., Mitani, F., Agake, R., and Ishimura, Y. (1998) *Eur. J. Biochem.* **256,** 190–200
25. Mukai, K., Nagasawa, H., Agake-Suzuki, R., Mitani, F., Totani, K., Yanai, N., Obinata, M., Suematsu, M., and Ishimura, Y. (2002) *Eur. J. Biochem.* **269,** 69–81
26. Obinata, M. (1997) *Genes Cells* **2,** 235–244
27. Obinata, M. (2001) *Biochem. Biophys. Res. Commun.* **286,** 667–672
28. Schimmer, B. P. (1979) *Methods Enzymol.* **58,** 570–574
29. Mukai, K., Imai, M., Shimada, H., Okada, Y., Ogishima, T., and Ishimura, Y. (1991) *Biochem. Biophys. Res. Commun.* **180,** 1187–1193
30. Mukai, K., Imai, M., Shimada, H., and Ishimura, Y. (1993) *J. Biol. Chem.* **268,** 9130–9137
31. Domalik, L. J., Chaplin, D. D., Kirkman, M. S., Wu, R. C., Liu, W. W., Howard, T. A., Seldin, M. F., and Parker, K. L. (1991) *Mol. Endocrinol.* **5,** 1853–1861
32. Ogishima, T., Suzuki, H., Hata, J., Mitani, F., and Ishimura, Y. (1992) *Endocrinology* **130,** 2971–2977
33. Kozak, M. (1987) *Nucleic Acids Res.* **15,** 8125–8148
34. von Heijne, G. (1984) *J. Mol. Biol.* **173,** 243–251
35. Wex, T., Lipyansky, A., Bromme, N. C., Wex, H., Guan, X. Q., and Bromme, D. (2001) *Biochemistry* **40,** 1350–1357
36. Nelson, T. R., Charonis, A. S., McIvor, R. S., and Butkowski, R. J. (1995) *J. Biol. Chem.* **270,** 16265–16270
37. Kanwar, Y. S., Kumar, A., Yang, Q., Tian, Y., Wada, J., Kashihara, N., and Wallner, E. I. (1999) *Proc. Natl. Acad. Sci. U. S. A.* **96,** 11323–11328
38. Ikeda, M., Takemura, T., Hino, S., and Yoshioka, K. (2000) *Biochem. Biophys. Res. Commun.* **268,** 225–230
39. The *Caenorhabditis elegans* Sequencing and Consortium (1998) *Science* **282,** 2012–2018
40. Smas, C. M., and Sul, H. S. (1993) *Cell* **73,** 725–734
41. Halder, S. K., Takemori, H., Hatano, O., Nonaka, Y., Wada, A., and Okamoto, M. (1998) *Endocrinology* **139,** 3316–3328
42. Okamoto, M., Takemori, H., Halder, S. K., Nonaka, Y., and Hatano, O. (1998) *Endocr. Res.* **24,** 515–520
43. Raza, F. S., Takemori, H., Tojo, H., Okamoto, M., and Vinson, G. P. (2001) *Eur. J. Biochem.* **268,** 2141–2147
44. Laird, S. M., Vinson, G. P., and Whitehouse, B. J. (1988) *Acta Endocrinol.* **119,** 420–426
45. Raza, F. S., Puddefoot, J. R., and Vinson, G. P. (1998) *Endocr. Res.* **24,** 977–981
46. Kalfa, T. A., Thull, J. D., Butkowski, R. J., and Charonis, A. S. (1994) *J. Biol. Chem.* **269,** 1654–1659
47. Kamphuis, I. G., Drenth, J., and Baker, E. N. (1985) *J. Mol. Biol.* **182,** 317–329
48. Vernet, T., Khouri, H. E., Laflamme, P., Tessier, D. C., Musil, R., Gour-Salin, B. J., Storer, A. C., and Thomas, D. Y. (1991) *J. Biol. Chem.* **266,** 21451–21457
49. Baker, S. C., Yokomori, K., Dong, S., Carlisle, R., Gorbalenya, A. E., Koonin, E. V., and Lai, M. M. (1993) *J. Virol.* **67,** 6056–6063
50. Iannaccone, P. M., and Weinberg, W. C. (1987) *J. Exp. Zool.* **243,** 217–223
51. Morley, S. D., Viard, I., Chung, B. C., Ikeda, Y., Parker, K. L., and Mullins, J. J. (1996) *Mol. Endocrinol.* **10,** 585–598

ELSEVIER

Biochimica et Biophysica Acta 1619 (2003) 317–324

BIOCHIMICA ET BIOPHYSICA ACTA
BBA

www.bba-direct.com

Review

The undifferentiated cell zone is a stem cell zone in adult rat adrenal cortex

Fumiko Mitani*, Kuniaki Mukai, Hirokuni Miyamoto, Makoto Suematsu, Yuzuru Ishimura[1]

Department of Biochemistry, School of Medicine, Keio University, 35 Shinanomachi, Shinjuku-ku, Tokyo 160-8582, Japan

Received 25 March 2002; accepted 23 October 2002

Abstract

The adrenal cortex of mammals has been known to consist of three morphologically and functionally distinct zones, i.e. the zona glomerulosa (zG), the zona fasciculata (zF) and the zona reticularis (zR), each of which secretes a specific corticosteroid different from those produced by the other two zones. We found previously, however, that an additional zone existed between zG and zF of adult rat adrenal cortex and that the cells in that zone were in a functionally undifferentiated state as an adrenocortical cell [Endocrinology 135, (1994) 431]: they were incapable of synthesizing highly active forms of corticosteroids, such as aldosterone and corticosterone, although they could produce their precursors. Hence, we named the zone as the undifferentiated cell zone (zU) of the adrenal cortex. Here we show that zU and its surroundings, i.e. the innermost portion of zG and the outermost portion of zF are the sites for cell replication in adult rat adrenal cortex and that the cells raised there migrate to other regions. Such cell replications in this region occur regardless of physiological conditions, such as the rise and fall of hormonal stimuli and circadian fluctuation of adrenocortical activities. On the bases of these and other findings previously described, we propose that zU is the stem cell zone of the adult rat adrenal cortex. Our recent success in isolating novel cell lines, which display an undifferentiated phenotype similar to that of zU cells, could facilitate the exploration of molecular mechanisms for the differentiation and development of the adrenocortical cells.
© 2002 Elsevier Science B.V. All rights reserved.

Keywords: Stem cell; Adrenal cortex; Circadian rhythm; Cell differentiation; Steroidogenesis; Cytogenesis

The adrenal glands are composed of two functionally and ontogenetically different tissues, the medulla and the cortex. The cortex, the subject of the present article, further consists of three concentric zones, the zona glomerulosa (zG), the zona fasciculata (zF), and the zona reticularis (zR). zG cells produce mineralocorticoids, such as aldosterone under the control of the renin–angiotensin system, while zF cells secrete glucocorticoids under the regulation of ACTH, an anterior pituitary hormone. The principal glucocorticoid varies in animals depending on the species; it is cortisol in human and other primates, whereas it is corticosterone in many rodents. zR cells of primates, including humans, secrete adrenal androgens such as dehydroepiandrosterone (DHAS). Thus, cells in each zone have an endocrine function unique to the individual zone, and this phenomenon is called as the "functional zonation" of the adrenal cortex [1–7].

Later, however, we found another cell zone between zG and zF of adult rat adrenal cortex [8]. The cells in this zone were determined not to secrete highly active and differentiated forms of corticosteroid such as aldosterone, corticosterone and DHAS, and yet are considered to be the adrenocortical parenchymal cells. They contained SF-1/Ad4BP, a steroidogenic tissue-specific transcription factor [9,10], and other marker proteins present in adrenocortical cells, including cytochrome P450scc [11] and 3β-hydroxy steroid dehydrogenase [12]. We designated the cell zone as the undifferentiated cell zone (zU) of the adrenal cortex. The present article will summarize, though briefly, our past and ongoing efforts to explore the function and/or physiological significance of this newly discovered zone.

1. Properties of the undifferentiated cell zone

Fig. 1 shows the double immunohistochemical staining of rat adrenal gland with antibodies against zone-specific steroidogenic enzymes [13,14], i.e. aldosterone synthase cytochrome P450 (P450aldo) for zG and steroid 11β-

* Corresponding author. Tel.: +81-3-5363-3752; fax: +81-3-3358-8138.
E-mail address: fmitani@sc.itc.keio.ac.jp (F. Mitani).
[1] Present address: The Department of Biochemistry, The University of Texas Health Science Center at San Antonio, San Antonio, TX 78229-3900, USA.

0304-4165/02/$ - see front matter © 2002 Elsevier Science B.V. All rights reserved.
PII: S0304-4165(02)00490-7

hydroxylase (P45011β) for zF [8]. As seen, there is a new zone consisting of five to six cell layers between P450aldo-positive zG (blue) and P45011β-positive zF (brown), and the fact that the zone has no color indicates the absence of both P450aldo and P45011β, which catalyze the formation of aldosterone and corticosterone, respectively. Since adrenal glands of animals such as rats and mice are devoid of cytochrome P45017α,lyase [3,5,15], which catalyzes the formation of adrenal androgens in zR of many mammals [16], the zone can be characterized as lacking adrenal androgen synthesis as well, and hence any highly developed form of adrenocortical steroid hormones. In other words, the cells in this zone have no differentiated adrenocortical function so far recognized and, therefore, have been designated as the undifferentiated cell zone (zU) [8].

Further histological examination of the new zone revealed well-packed nuclei and small amounts of lipids in these cells, as compared to those in the other cortical zones [8,17]. As judged from these observations, the zone might be the same as the "zona intermedia", "transitional zone" or "sudanophobe zone", described previously based upon histologic views [18–21]. We then studied cell replication in this zone by examining S-phase cells with incorporation of 5′ -bromo-deoxyuridine (BrdU) to their nuclei and by detecting proliferating cell nuclear antigen (PCNA) and/or mitotic figures of cells [8,22,23]. Fig. 2 shows such distribution of BrdU-labeled cells in the adrenal cortex; they are rich in and around zU. PCNA-expressing cells were also found in zU and its neighborhood. Since S-phase cells were scarcely found in the other regions of the adrenal cortex, zU and its surroundings must be the site of cell proliferation in adult rat adrenal cortex.

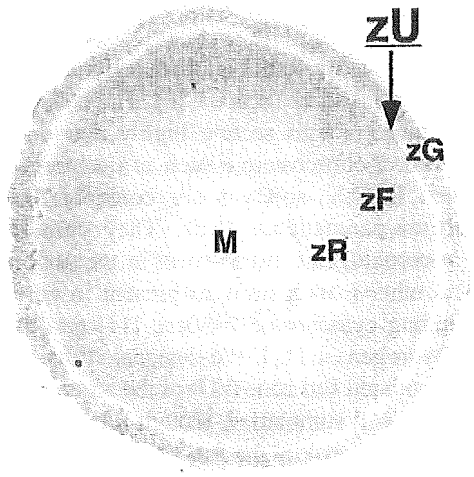

Fig. 1. New zone of rat adrenal cortex. The single adrenal section of the rat (Sprague–Dawley rats, male, about 200 g body weight) fed on sodium (Na)-deficient diet (8.6 mmol equivalent Na/kg diet) for 20 days was stained simultaneously with anti-P450aldo and anti-P45011β antibodies. For details, see Ref. [8]. Note that P450aldo (blue) is confined to zG and P45011β (brown) to zF. A colorless zone in between zG (blue) and zF (brown) is designated as the undifferentiated cell zone (zU). zG, the zona glomerulosa; zF, the zona fasciculata; zR, the zona reticularis; M, the medulla.

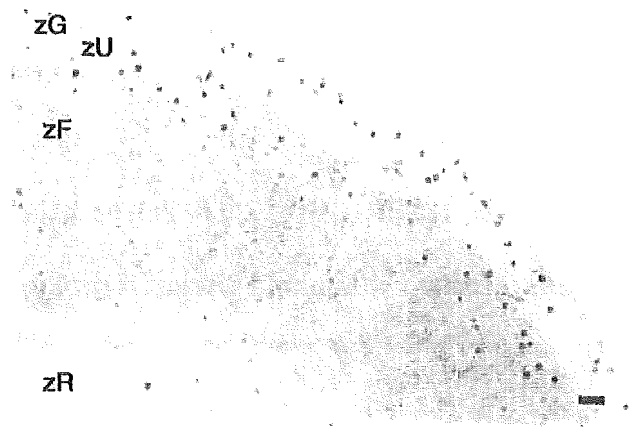

Fig. 2. Spatial distribution of BrdU-labeled cells in the adrenal cortex. BrdU (50 mg BrdU/ kg body weight) was injected i.p. to adult rats under normal dietary conditions 1 h before sacrifice at 4 a.m. Black dots represent BrdU-incorporated nuclei in S-phase cells. The section was also stained with anti-P45011β antibody to show the portion of zF and delineate the inner edge of zU. zG, the zona glomerulosa; zF, the zona fasciculata; zR, the zona reticularis; zU, the undifferentiated cell zone. Bar = 50 μm.

2. Circadian changes in cell proliferation

We next studied the temporal distribution of BrdU-labeled cells in the adrenal cortex, since we observed changes in total numbers of replicating cells in the adrenal cortex, depending on the time of BrdU injection to the rats. It also has been reported that the cell replication in tissues such as the cornea of the eyes, epidermis and gastrointestinal tract shows diurnal variations [24,25]. As seen in Fig. 3A, the number of BrdU-labeled cells in the adrenal cortex exhibited a marked fluctuation depending on clock-time with a maximum at 4 a.m. [22,23]. Cells expressing PCNA showed their highest peaks also at around 4 a.m. with a similar temporal pattern to that shown in Fig. 3A. Thus, the cell proliferation in the adrenal cortex has a circadian rhythm. Furthermore, it was noticed that BrdU-labeled cells were always present in zU and its surroundings, i.e. the innermost portion of zG and the outermost portion of zF [22,23,26]. Among them, the outermost portion of zF was most rich in replicating cells, which reached their highest number at 4 a.m., the peak time of the circadian rhythm (Fig. 3B, open squares).

3. Roles of ACTH and renin–angiotensin systems in cell proliferation

It is well known that ACTH affects growth and endocrine function in the adrenal cortex. Furthermore, the plasma concentration of ACTH itself exhibits a circadian rhythm [1]. We accordingly examined whether the circadian rhythm

in the adrenocortical cell proliferation was correlative to the plasma ACTH concentration, and found that the peak in replication of the adrenocortical cells was preceded by 4 h with the peak of plasma ACTH concentration [22]. When the peak of plasma ACTH concentration was forced to shift temporally by treating the animal with exogenous ACTH or with certain other drugs, the rhythm of cell replication was found to shift accordingly [22]. Thus the rise in plasma ACTH concentration seems to trigger the cell replication, especially that in the outermost portion of zF. Further study is necessary however to clarify the regulatory mechanisms of cell replication and other activities of the adrenal cortex by ACTH [27].

In the innermost portion of zG, on the other hand, elevation in plasma ACTH concentration had little effect on the cell replication, suggesting the cytogenesis in this region was regulated by a different mechanism from the ACTH-related one [28]. When the effects of renin–angiotensin system were examined by feeding the animals with a Na-deficient diet [28,29], the cell replication increased significantly in the innermost portion of zG with a peak at around 8 p.m. ($P<0.01$) (closed squares in Fig. 3B and black columns in Fig. 3C). It is well-known that Na-deficiency results in an activation of the renin–angiotensin system, which in turn increases the proliferation of zG cells along with expression of P450aldo [8,14,30,31]. Under Na-normal diet, the number of replicating cells in zG was considerably smaller than that in the outermost portion of zF, and the circadian rhythm was hardly observable (Fig. 3C, white columns). The increment at 8 p.m. under Na-deficiency was diminished by administration of Losartan, an antagonist of angiotensin receptor type 1, but not by PD 123319, an antagonist of the receptor type 2 [32]. Therefore, the increase in the cell replication at 8 p.m. was thought to occur via angiotensin receptor type 1. These observations demonstrated that the cell replication in two regions around zU, i.e. the outermost portion of zF and the innermost portion of zG, are regulated mainly by ACTH stimuli and the renin–angioten-

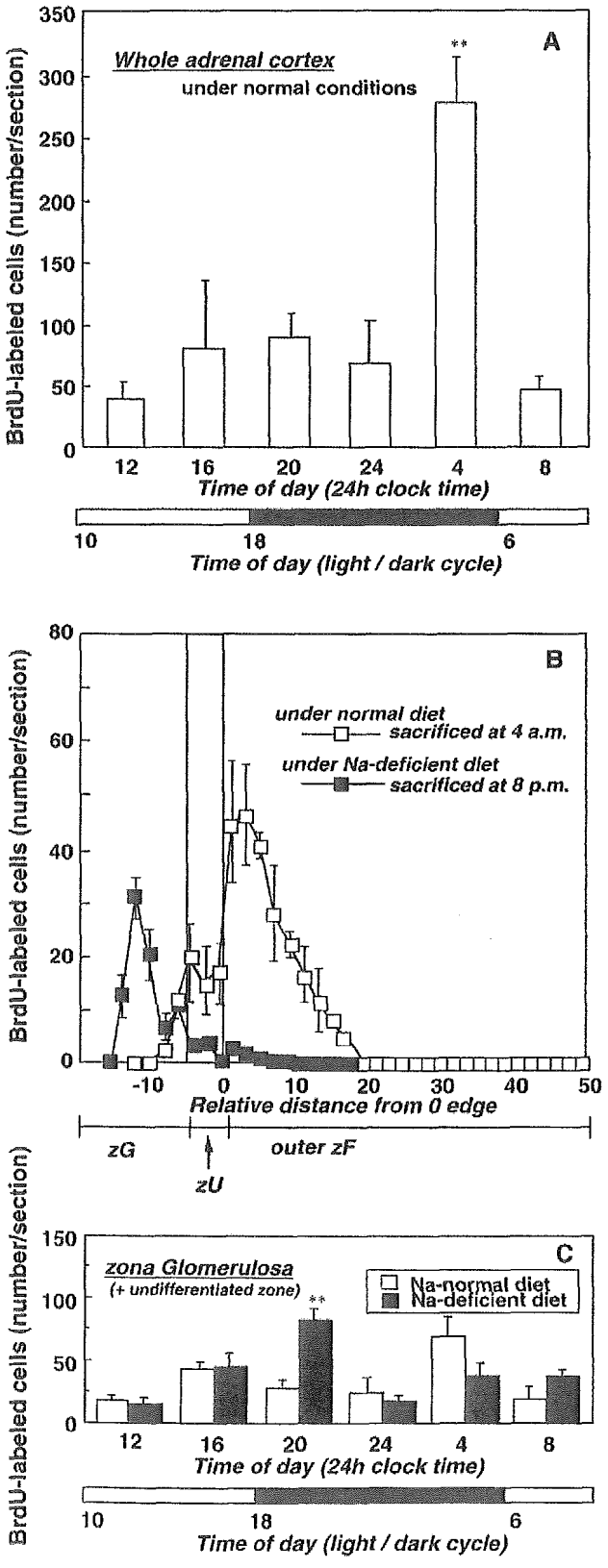

Fig. 3. Circadian rhythm in the cell proliferation. (A) Circadian rhythm in the number of BrdU-labeled cells in a whole adrenal cortex from rats under normal dietary conditions. $^{**}P<0.01$; data at 4 a.m. vs. at other hours. The time of day (light/dark cycle) below the X-axis shows the light (white portion) and dark duration (black portion) in a day. (B) Spatial distribution of BrdU-labeled cells in the adrenal cortex: (□) BrdU-labeled cells in the adrenal cortex from rats fed on Na-normal diet (86 mmol equivalent Na/kg diet) for 10 days and sacrificed at 4 a.m., (■) BrdU-labeled cells in the adrenal cortex from rats fed on Na-deficient diet (8.6 mmol equivalent Na/kg diet) for 10 days and sacrificed at 8 p.m. Numbers on the X-axis (relative distance from 0 edge) show the distance (cell layer) from "0" which is defined as the position of the innermost cell layer of the undifferentiated cell zone in the adrenal cortex. Each point shows the total number of BrdU-positive nuclei within two cell layers and is plotted against "relative distance from 0 edge". zG, the zona glomerulosa; outer zF, outer zona fasciculata; zU, the undifferentiated cell zone. (C) Circadian rhythm in the cell proliferation in the zG of rats fed on either Na-normal or Na-deficient diets for 10 days. $^{**}P<0.01$, data at 8 p.m. (20 of 24 h clock time) of Na-deficient rats vs. that of Na-normal rats. The rats were injected with BrdU as described in the legend for Fig. 2 at 1 h before sacrifice at indicated time of a day. The BrdU-labeled cell-nuclei were counted in about 30 sections (6 μm frozen sections) from 9–10 different adrenal cortices (about five rats) at each time point and statistically analyzed using one- and two-way ANOVA followed by the post hoc Dunn's Procedure. Values are mean ± S.E. ($n=5$). For details, see Refs. [8,22].

sin system, respectively, with circadian rhythms different from each other. It should be noted here that BrdU-labeled cells were always detectable in zU even under Na-deficient conditions, though very small in number.

4. Migration of BrdU-labeled cells to other regions

The behavior of BrdU-labeled cells, i.e. that of the DNA-synthesizing cells, was examined from 1 h to 20 days after the injection of BrdU [8,17]. Fig. 4 shows the results from the pulse-chase experiments in which BrdU was injected to rats at 11 a.m., under normal hormonal conditions, and examined at appropriate time points. One hour after the injection, BrdU-labeled cells were found in and around zU (Fig. 4A) as described in the previous section. After 20 days, the cells labeled with BrdU were found to shift to the inner portion of zF (compare Fig. 4B with Fig. 4A), indicating that the BrdU-labeled cells migrated centripetally under ordinary hormonal conditions. Here it should be noted that the number of the BrdU-labeled cells increased by about 3-fold after 20 days,

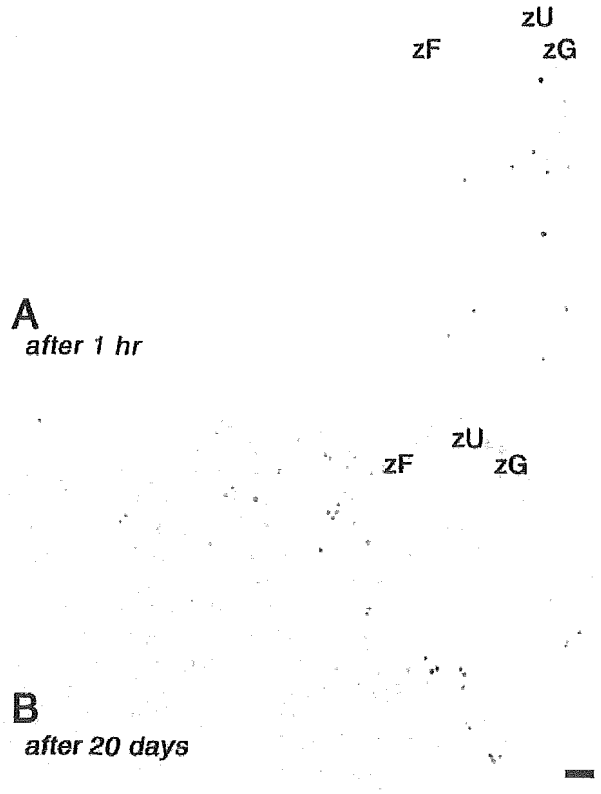

Fig. 4. Migration of BrdU-labeled cells under normal dietary conditions. (A) Localization of BrdU-labeled cells in the adrenal cortex at 1 h after the injection of BrdU. (B) Localization of BrdU-labeled cells in the adrenal cortex at 20th day after the injection of BrdU. Rats fed on Na-normal diet was injected with BrdU at 11 a.m. and sacrificed 1 h (A) or 20 days thereafter (B). Black dots show BrdU-labeled nuclei in cells. Nuclei (gray dots) were post-stained with 0.1% hematoxylin. For details, see Refs. [8,17]. zG, the zona glomerulosa; zF, the zona fasciculata; zU, the undifferentiated cell zone. Bar = 100 μm.

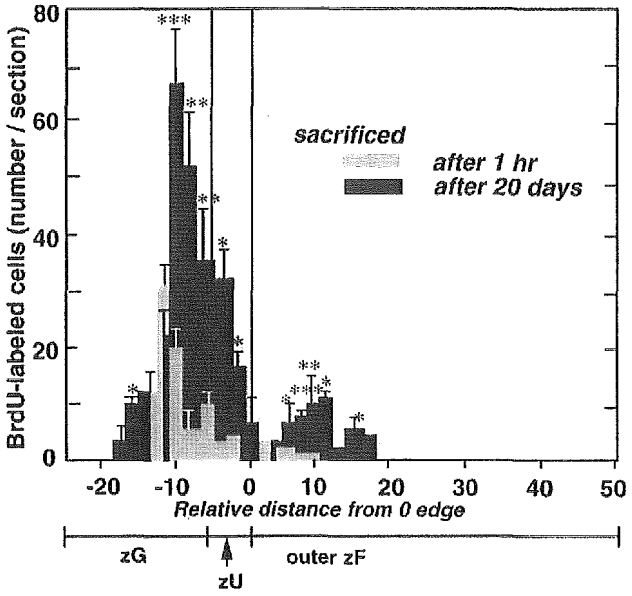

Fig. 5. Behavior of BrdU-labeled cells under sodium-deficiency. Rats were fed on Na-deficient diet for 10 days as described in the legend for Fig. 3. BrdU was then injected at 7 p.m. and the rats were sacrificed at 1 h (gray column) or at the 20th day (black column) after the injection. Rats were maintained with Na-deficient diet during the experiment. For details, see Ref. [29]. Numbers on the *X*-axis show the distance from "0" as described in the legend for Fig. 3. zG, the zona glomerulosa; outer zF, outer zona fasciculata; zU, the undifferentiated cell zone. $^{*}P<0.05$, $^{**}P<0.01$, $^{***}P<0.001$: data obtained at 1 h vs. at the 20th day in a comparable region, all determined as described in the legend for Fig. 3. Values are mean ± S.E. ($n=5$).

indicating that further cell divisions had occurred during the migration. Then behavior of cells labeled with BrdU at 7 p.m. under Na-deficiency was also examined [29]. As shown in Fig. 5 (gray columns), cells labeled under the conditions were found mostly in the innermost portion of zG with a few in zU, at 1 h after the incorporation. Thereafter, they did not move greatly and, even at the 20th day after the administration (Fig. 5, black columns), they were still within the same area (zG and zU). The number of labeled cells increased again by about 3-fold during the 20-day period, indicating that they further proliferated within that time. A small population of cells found in the outer zF were probably those that migrated from the outermost portion of zF.

Thus, BrdU-labeled cells in the two regions around zU seemed to behave differently, i.e. BrdU-labeled cells in the outermost portion of zF migrated centripetally with days, while those in the innermost portion of zG and in zU had not migrated elsewhere even 20 days after the administration of BrdU.

5. A proposed mechanism for the cell supply in the adrenal cortex

Fig. 6 shows our hypothesis on the mechanisms for cell replenishment in the adrenal cortex [33]. Here, zU is the

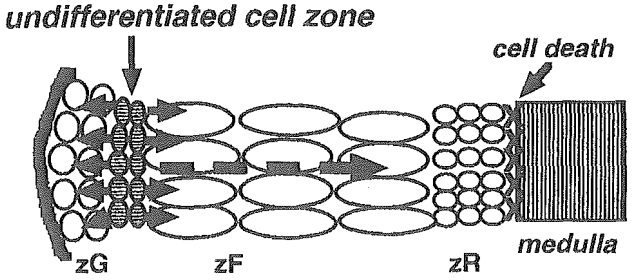

Fig. 6. Proposed mechanism for the cell renewal and maintenance. The undifferentiated cell zone could be a stem cell zone that provides cells differentiating into zone-specific cells. Cells differentiating to the zF cells migrate inwardly and then transform into the zR cells. They finally degenerate at the border between the cortex and the medulla. Meanwhile, the fate of cells differentiating into zona glomerulosa cells may be within the zona glomerulosa. (◎) Cells in the undifferentiated cell zone; (—►) replenishing of cells in the undifferentiated zone to the zona glomerulosa and to the zona fasciculata-reticularis cells; (---►) cell migration; (×) cell death. zG: the zona glomerulosa. zF: the zona fasciculata, zR: the zona reticularis.

stem cell zone in the adult rat adrenal cortex, providing cells which differentiate into zG, zF and zR cells (Fig. 6, short black arrows). The replenished cells in the outermost portion of zF proliferate, migrate inwards (Fig. 6, long arrows with broken lines), differentiate into zF and zR cells during the migration, and degenerate at the edge of the medulla, where most of the cortical cells are considered to die by apoptosis [34–36]. Cells to differentiate into zG cells, on the other hand, may contribute to maintain only zG and die without migrating out toward the other zones (refer to Fig. 5). In this regard, it is interesting to note that, in human adrenal cortex, apoptotic cells have also been detected in the outermost portion of the adrenal cortex [37].

The above described processes for replenishing the cells in the adrenal cortex resemble the replacement processes of epithelial cells in small intestine [38]. The crypt of small intestine contains a ring of stem cells located at the fourth position from the bottom and, just above the ring, there are many cells that are more actively proliferating than the stem cells. Those proliferated cells migrate up to the villus with differentiation and are extruded at the villus tip as apoptotic cells.

6. Novel cell lines displaying the phenotype similar to that of the undifferentiated cell zone

We have recently established three adrenocortical cell lines, AcA101, AcA201 and AcE60, from adrenal glands of adult transgenic mice harboring a temperature-sensitive SV40 T-antigen gene (Fig. 7) [39]. It should be mentioned here that zU is present not only in the rat adrenal cortex but also in that of mouse [39] and possibly in the adrenal

cell line	expression of specific mRNA molecules					
	SF-1	P450scc	P45011β			P450aldo
	33°C	33°C	33°C	39°C	39°C + Bt_2 cAMP	33°C & 39°C
AcA 101	+	+	-	-	+	-
AcA 201	+	+	+	+	+	-
AcE 60	+	+	-	+	+	-

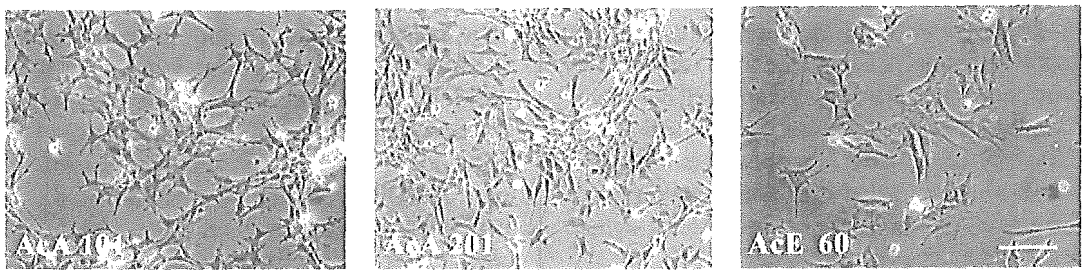

Fig. 7. Established adrenocortical cell lines from the adrenal gland of adult transgenic mice harboring the temperature-sensitive SV40 T-antigen gene. Cell lines were obtained from a primary culture of the adrenal glands from transgenic mice carrying a ts mutant of SV40 large T-antigen gene tsA58 [39]. Cells were cultured in the media (DMEM/F-12 or RITC80-7) containing 15% horse serum, 2.5% fetal bovine serum and penicillin/streptomycin. To identify the expression of SF-1/Ad4BP, P450scc, P45011β and P450aldo mRNAs [48,49], RT-PCR analyses were performed with specific oligonucleotide primer pairs for each molecule after cDNAs were synthesized with reverse transcriptase [50,51]. For details, see Ref. [39]. (33 °C) Cultured at 33 °C; (39 °C) cultured at 39 °C; (39 °C + Bt_2cAMP) cultured at 39 °C in the presence of 1 mM Bt_2cAMP (dibutylyl cAMP); (+) mRNA is detectable; (−) mRNA is undetectable. Phase contrast micrographs at the bottom of this figure show morphological features of three cell lines, AcA101, AcA201 and AcE60. Cells were cultured at subconfluent stages at the permissive temperature (33 °C) for the ts SV40 T-antigen. Bar = 50 μm.

cortices of other animals. Morphological features as well as their expression patterns of steroidogenic proteins in these cell lines are depicted in Fig. 7. As seen, AcA101 and AcA201 cells display retracted appearances, while AcE60 cells show a larger and flatter appearance being less retracted than AcA101 and AcA201 cells.

All three cell lines mentioned above express mRNAs of steroidogenic factor-1 (also called Ad4BP) [9,10] and P450scc, suggesting that they all derive from parenchymal cells of the adrenal cortex or have the same origin with parenchymal cells. Among them, AcA101 and AcE60 displayed a similar pattern of steroidogenic gene expression to that of zU, i.e. no expression of P450aldo and P45011β mRNAs at the permissive temperature (33 °C) for SV40 T-antigen. Interestingly AcE60 and AcA101 cells were capable of differentiating into zF-like cells which express P45011β at 39 °C (non-permissive temperature for the SV40 T-antigen) in the absence and presence of dibutylyl cAMP, respectively. AcA201 cells are the zF-like cells expressing P45011β mRNA at 33 °C [39]. Although we have so far not been successful in differentiating such undifferentiated cells, AcA101 and AcE60 cells, to P450aldo mRNA-expressing zG-like cells, these cell lines may serve as useful tools to investigate the differentiation mechanism(s) of the adrenocortical cells.

7. Remarks

Mechanisms for cell renewal and structural maintenance of the adult adrenal cortex have been an important subject in the physiology of the adrenal gland [40,41] and hence in endocrinology. One of the early hypotheses on the maintenance of the adrenal cortex is "cell migration theory", proposed by Gottschau in 1883 [42]. In this proposal, adrenocortical cells are supposed to be born immediately below the capsule and migrate centripetally with differentiation to zG, zF and zR cells. This means that a single site (or a region) is capable of reproducing all cortical parenchymal cells in three different zones. This theory has been supported by many workers (as reviewed in Ref. [8] and Refs. [40,41]) including Zajicek et al. [43] and Morley et al. [44]. An opposing hypothesis to the cell migration theory is the "zonal theory" by Chester-Jones [45] in 1948, though supported by only a small number of investigators (see Refs. [40,41]). It claims that each zone replenishes its own cells independently, implicating at least three sites in providing cells for the three zones.

As described, our results presented here have shown that the cell division occurs at an area consisted of zU and its surroundings, and the cells born there are provided to the three zones. Then, further insight into the area revealed that cell proliferation is more active in the two regions which sandwich zU, i.e. the innermost region of zG and the outermost region of zF, than in zU itself. Available evidence indicated that the former provides cells to zG under regulation by the renin–angiotensin system and the latter replenishes cells to both zF and zR under control of ACTH. In this respect, our findings disagree with both "cell migration theory" and "zonal theory", but are consistent with the "proliferative intermediate zone hypothesis" of Idelman [46]. He has proposed that cells in "the intermediary zone" between zG and zF provide daughter cells to both zG and zF, where the intermediary zone might correspond to zU and its surroundings described in this article. Beyond these discussions, however, we were able to discover zU, i.e. undifferentiated cell zone without terminal corticosteroid synthesizing enzymes, and also able to recognize two distinct cell-proliferating regions in both sides of zU. On the basis of these findings and foregoing discussions on the stem cell zones of epithelial cells [38], we strongly suggest here that zU serves as the stem cell zone of the adult rat adrenal cortex. Whether zG cells and zF and zR cells arise from a single kind of stem cell or two different stem cells in zU and what kinds of factors stimulate the differentiation of the stem cell into the two major types of adrenocortical cells remain to be answered.

Finally, it should be emphasized that the situation described above is entirely different from that of the fetal adrenal gland [34,44]. In the fetal adrenal gland, which is developing rapidly, the cortical cells are all zF-like cells expressing P45011β and are intermingled with the medulla cells [34,47]. No cortical zonation nor zU was observed, and replicating cells (BrdU-labeled cells) were scattered over the whole growing adrenal gland. It is only after birth, when the cortical zonation including zU was established, the stem cells being concentrated in zU [34,47]. Further investigation is obviously necessary to determine the molecular mechanisms of the cell replenishment and maintenance of adult adrenal cortex, as well as of the development and differentiation of the adrenocortical cells.

Acknowledgements

We thank Dr. J. Hata and Dr. H. Suzuki of Keio University for the advice for immunohistochemical studies and Dr. N. Yanai and Dr. M. Obinata of Tohoku University for kindly providing transgenic mice harboring the temperature-sensitive SV40 T-antigen gene and fruitful discussions during the study. Antibodies against P45017α,lyase and Ad4BP were generous gifts of from Dr. S. Kominami of Hiroshima University and Dr. K. Morohashi of National Institute for Basic Biology, Okazaki, Japan, respectively. We also thank Dr. Bettie Sue S. Masters of the University of Texas Health Science Center at San Antonio, TX, USA for her kind aid during the preparation of this manuscript. Finally, excellent technical assistance of Mr. T. Ogawa, Ms. C. Motomura and Ms. M. Kondo is greatly acknowledged.

This work was supported in part by Grants-in-aid for General Scientific Research from the Ministry of Education,

Science and Culture, Japan and by grants from the Mitsubishi Foundation, Uehara Memorial Foundation, Tanabe Science Foundation and Keio University.

References

[1] D.N. Orth, W.J. Kavacs, D.C. Rowan, The adrenal cortex, in: J.D. Wilson, D.W. Foster (Eds.), William's Textbook of Endocrinology, Saunders, Philadelphia, 1992, pp. 489–619.

[2] J. Arnold, Ein Beitrag zu der feineren Structur und dem Chemismus der Nebennieren, Virchows Arch. 35 (1866) 64–107.

[3] P.J. Hornsby, The regulation of adrenocortical function by control of growth and structure, in: D.C. Anderson, J.S.D. Winter (Eds.), The Adrenal Cortex, Butterworths & Co., London, 1985, pp. 1–31.

[4] J. Stachenko, C.J.P. Giroud, Further observations on the functional zonation of the adrenal cortex, Can. J. Biochem. 42 (1964) 1777–1785.

[5] S. Takemori, S. Kominami, The role of cytochrome P450 in adrenal steroidogenesis, Trends Biochem. Sci. 9 (1984) 393–396.

[6] F. Mitani, Cytochrome P450 in adrenocortical mitochondria, Mol. Cell. Biochem. 24 (1979) 21–43.

[7] W.L. Muller, Molecular biology of steroid hormone synthesis, Endocr. Rev. 9 (1988) 295–318.

[8] F. Mitani, H. Suzuki, J. Hata, T. Ogishima, H. Shimada, Y. Ishimura, A novel cell layer without corticosteroid-synthesizing enzymes in rat adrenal cortex: histochemical detection and possible physiological role, Endocrinology 135 (1994) 431–438.

[9] X. Luo, Y. Ikeda, K.L. Parker, A cell-specific nuclear receptor is essential for adrenal and gonadal development and sexual differentiation, Cell 74 (1994) 481–490.

[10] K. Morohashi, H. Iida, M. Nomura, O. Hatano, S. Honda, T. Tsukiyama, O. Niwa, T. Hara, A. Takakusu, Y. Shibata, T. Omura, Functional difference between Ad4BP and ELP, and their distribution in steroidogenic tissues, Mol. Endocrinol. 8 (1994) 643–653.

[11] F. Mitani, T. Shimizu, R. Ueno, Y. Ishimura, S. Izumi, N. Komatsu, K. Watanabe, Cytochrome P45011β and P450scc in adrenal cortex; Zonal distribution and intramitochondrial localization by the horseradish peroxidase-labeled antibody method, J. Histochem. Cytochem. 30 (1982) 1066–1074.

[12] H. Sasano, J.I. Mason, N. Sasano, H. Nagura, Immunolocalization of 3β-hydroxysteroid dehydrogenase in human adrenal cortex and in its disorders, Endocr. Pathol. 1 (1990) 94–101.

[13] T. Ogishima, F. Mitani, Y. Ishimura, Isolation of aldosterone synthase cytochrome P450 from zona glomerulosa mitochondria of rat adrenal cortex, J. Biol. Chem. 264 (1989) 10935–10938.

[14] T. Ogishima, H. Suzuki, J. Hata, F. Mitani, Y. Ishimura, Zone-specific expression of aldosterone synthase cytochrome P450 and cytochrome P45011β in rat adrenal cortex: histochemical basis for the functional zonation, Endocrinology 130 (1992) 2971–2977.

[15] C. Laplante, C.J.P. Giroud, J. Stachenko, Lack of appreciable 17α-hydroxylase activity in the normal and regenerated rat adrenal cortex, Endocrinology 75 (1964) 825–827.

[16] K. Shinzawa, S. Ishibashi, M. Murakoshi, K. Watanabe, S. Kominami, A. Kawahara, S. Takemori, Relationship between zonal distribution of microsomal cytochrome P450s (P45017α,lyase and P450c21) and steroidogenic activities in guinea-pig adrenal cortex, J. Endocrinol. 119 (1988) 191–200.

[17] F. Mitani, T. Ogishima, H. Miyamoto, Y. Ishimura, Localization of P450aldo and P45011β in normal and regenerating rat adrenal cortex, Endocr. Res. 21 (1995) 413–423.

[18] H.W. Deane, R.O. Greep, A morphological and histochemical study of the rat's adrenal cortex after hypophysectomy, with comments on the liver, Am. J. Anat. 79 (1946) 117–145.

[19] D.B. Carter, J.D. Lever, The zona intermedia of the adrenal cortex. A correlation of possible functional significance with development morphology and histochemistry, J. Anat. 88 (1954) 437–454.

[20] A.J. Cain, R.G. Harrison, Cytological and histochemical variations in the adrenal cortex of the albino rat, J. Anat. 84 (1950) 196–226.

[21] R.M. Mitchell, Histological changes and mitotic activity in the rat adrenal during postnatal development, Anat. Rec. 101 (1984) 161–185.

[22] H. Miyamoto, F. Mitani, K. Mukai, M. Suematsu, Y. Ishimiura, Studies on cytogenesis in adult rat adrenal cortex: circadian and zonal variations and their modulation by adrenocorticotropic hormone, J. Biochem. (Tokyo) 126 (1999) 1175–1183.

[23] Y. Ishimura, F. Mitani, K. Mukai, H. Miyamoto, M. Suematsu, A functionally undifferentiated cell layer between the zona glomerulosa and the zona fasciculata of the adrenal cortex of rats: is it the stem cell zone? in: M. Okamoto, Y. Ishimura, H. Nawata (Eds.), Molecular Steroidogenesis, Universal Academic Press, Tokyo, 2000, pp. 201–204.

[24] R. Smaaland, Circadian rhythm of cell division, Prog. Cell Cycle Res. 2 (1996) 241–266.

[25] W.R. Brown, A review and mathematical analysis of circadian rhythm in cell proliferation in mouse, rat, and human epidermis, J. Invest. Dermatol. 97 (1991) 273–280.

[26] F. Mitani, K. Mukai, H. Miyamoto, Localization of replicating cells in the rat adrenal cortex during the late gestational and early postnatal stages, Endocr. Res. 24 (1998) 983–986.

[27] C.E.P. Lotfi, Z. Todorovic, H.A. Armelin, B.P. Shimmer, Unmasking a growth-promoting effect of the adrenocorticotropic hormone in Y1 mouse adrenocortical tumor cells, J. Biol. Chem. 272 (1997) 29886–29891.

[28] H. Miyamoto, M. Mitani, K. Mukai, M. Suematsu, Y. Ishimura, Daily regeneration of rat adrenocortical cells: circadian and zonal variations in cytogenesis, Endocr. Res. 26 (2000) 899–904.

[29] H. Miyamoto, F. Mitani, K. Mukai, M. Suematsu, Y. Ishimura, A low-sodium diet affects the proliferation and migration of rat adrenocortical cells in vitro, in: M. Okamoto, Y. Ishimura, H. Nawata (Eds.), Molecular Steroidogenesis, Universal Academic Press, Tokyo, 2000, pp. 225–228.

[30] H. Shibata, T. Ogishima, F. Mitani, H. Suzuki, M. Murakami, T. Saruta, Y. Ishimura, Regulation of aldosterone synthase cytochrome P450 in rat adrenals by angiotensin II and potassium, Endocrinology 128 (1991) 2534–2539.

[31] M. Imai, T. Ogishima, H. Shimada, Y. Ishimura, Effect of dietary sodium restriction on mRNA for aldosterone synthase cytochrome P450 in rat adrenals, J. Biochem. (Tokyo) 111 (1992) 440–443.

[32] P.C. Wong, S.D. Hart, A.M. Zaspel, A.T. Chiu, P.J. Ardeckey, R.D. Smith, P.B. Timmermans, Functional studies of nonpeptide angiotensin II receptor subtype-specific ligands: DuP 753 (AII-1) and PD123177 (AII-2), J. Pharmacol. Exp. Ther. 255 (1990) 584–592.

[33] F. Mitani, K. Mukai, M. Suematsu, H. Miyamoto, Y. Ishimura, Fate of adrenocortical cells: distribution of degenerating cells and macrophages in the rat adrenal cortex, in: M. Okamoto, Y. Ishimura, H. Nawata (Eds.), Molecular Steroidogenesis, Universal Academic Press, Tokyo, 2000, pp. 231–232.

[34] F. Mitani, K. Mukai, H. Miyamoto, M. Suematsu, Y. Ishimura, Development of functional zonation in the rat adrenal cortex, Endocrinology 140 (1999) 3342–3353.

[35] S. Ceccatelli, A. Diana, M.J. Villar, P. Nicotera, Adrenocortical apoptosis in hypophysectomized rats is selectively reduced by ACTH, Neuroendocrinology 6 (1995) 342–345.

[36] R.V. Carsia, G.J. Macdonald, J.A. Gibney, K.I. Tilly, J.L. Tilly, Apoptotic cell death in rat adrenal gland: an in vivo and in vitro investigation, Cell Tissue Res. 283 (1996) 247–254.

[37] G.W. Wolkersdorfer, M.E. Bornstein, S. Brauer, C. Marx, W.A. Scherbaum, S.R. Bornstein, Differential regulation of apoptosis in the normal human adrenal gland, J. Clin. Endocrinol. Metab. 81 (1996) 4129–4136.

[38] C.S. Potten, M. Loeffler, Stem cells: attributes, cycles, spirals, pitfalls and uncertainties. Lessons for and from the crypt, Development 110 (1990) 1001–1020.

[39] K. Mukai, H. Nagasawa, R. Agake-Suzuki, F. Mitani, K. Totani, N.

Yanai, M. Obinata, M. Suematsu, Y. Ishimura, Conditionally immortalized adrenocortical cell lines at undifferentiated states exhibit inducible expression of glucocorticoid-synthesizing genes, Eur. J. Biochem. 269 (2002) 69–81.

[40] G.G. Nussdorfer, Cytogenesis in the rat adrenal cortex, in: G.H. Bourine, J.F. Danielli (Eds.), Cytophysiology of the Adrenal Cortex, International Review of Cytology, vol. 98, Academic Press, New York, 1986, pp. 319–330.

[41] M. Okamoto, H. Takemori, Differentiation and zonation of the adrenal cortex, Curr. Opin. Endocrinol. Diabetes 7 (2000) 122–127.

[42] M. Gottschau, Struktur und Embryonale Entwickellung der Nebennieren bei Saugetieren. Archiv Fur Anatomie und Entowickellungsgeschichte, Anatomischer Abteilung 9 (1883) 412–458.

[43] G. Zajicek, I. Ariel, N. Arber, The streaming adrenal cortex: direct evidence of centripetal migration of adrenocytes by estimation of cell turnover rate, J. Endocrinol. 111 (1986) 477–482.

[44] S.D. Morley, I. Viard, B.C. Chung, Y. Ikeda, K.L. Parker, J.J. Mullins, Variegated expression of a mouse steroid 21-hydroxylase/b-galactosidase transgene suggests centripetal migration of adrenocortical cells, Mol. Endocrinol. 10 (1996) 585–598.

[45] I. Chester-Jones, Variation in the mouse adrenal cortex with special reference to the zona reticularis and to brown degeneration together with discussion of the "cell migration" theory, Q. J. Microsc. Sci. 89 (1948) 53–73.

[46] S. Idelman, The structure of the mammalian adrenal cortex, in: I. Chester-Jones, I.W. Henderson (Eds.), General, Comparative and Clinical Endocrinology of the Adrenal Cortex, vol. 2, Academic Press, New York, 1978, pp. 1–199.

[47] F. Mitani, K. Mukai, T. Ogawa, H. Miyamoto, Y. Ishimura, Expression of cytochrome P450aldo and P45011β in rat adrenal gland during late gestational and neonatal stages, Steroids 62 (1997) 57–61.

[48] K. Mukai, M. Imai, H. Shimada, Y. Okada, T. Ogishima, Y. Ishimura, Structural differences in 5′-flanking regions of rat cytochrome P-450aldo and P-45011β genes, Biochem. Biophys. Res. Commun. 180 (1991) 1187–1193.

[49] K. Mukai, M. Imai, H. Shimada, Y. Ishimura, Isolation and characterization of rat CYP11B genes involved in late steps of mineralo- and glucocorticoid syntheses, J. Biol. Chem. 268 (1993) 9130–9137.

[50] K. Mukai, F. Mitani, H. Shimada, Y. Ishimura, Involvement of an AP-1 complex in zone-specific expression of the CYP11B1 gene in the rat adrenal cortex, Mol. Cell. Biol. 15 (1995) 6003–6012.

[51] K. Mukai, F. Mitani, R. Agake, Y. Ishimura, Adrenocorticotropic hormone stimulates CYP11B1 gene transcription through a mechanism involving AP-1 factors, Eur. J. Biochem. 256 (1998) 190–200.

Peyer's patch is the essential site in initiating murine acute and lethal graft-*versus*-host reaction

Masako Murai[1,2], Hiroyuki Yoneyama[1,2], Taichi Ezaki[3], Makoto Suematsu[4], Yuya Terashima[1], Akihisa Harada[1], Hiromasa Hamada[5], Hitoshi Asakura[2], Hiromichi Ishikawa[5] and Kouji Matsushima[1]

Published online 13 January 2003; doi:10.1038/ni879

Acute graft-*versus*-host disease (a-GVHD) is initiated primarily by immunologically competent cytotoxic T cells (CTLs) that express anti-host specificities. However, the host lymphoid compartment in which these precursor CTLs are initially stimulated remains unclear. Here we show that gut Peyer's patches (PPs) are required to activate anti-host CTL responses in a well characterized murine acute graft-*versus*-host reaction (a-GVHR) model, involving transfer of parent lymphocytes into F1 hybrid recipients. The a-GVHR was prevented when recruitment of donor T cells into PP was interrupted either by disrupting the gene encoding chemokine receptor CCR5 or by blocking integrin $\alpha_4\beta_7$–MAdCAM-1 (mucosal vascular addressin) interactions. Mice deficient for PPs failed to develop a-GVHD in two models of disease induction. Thus, blockade of CTL generation in PPs might offer new strategies for circumventing a-GVHD.

© 2003 Nature Publishing Group http://www.nature.com/natureimmunology

Acute graft-versus-host disease (a-GVHD) is one of the major obstacles of allogeneic bone marrow transplantation (BMT) used to treat patients with various lympho-hemopoietic malignancies[1,2]. Donor-derived, anti-host cytotoxic T cells (CTLs)[2–7] activated by host alloantigen-presenting cells (APCs)[4,8] have been implicated in the pathogenesis of a-GVHD, and the disease is characterized primarily by target epithelial organ injury[2,3,5,7–9]. The development of a-GVHD occurs in two phases *via* the transfer of donor lymphocytes. First, donor T cells encounter alloantigens expressed constitutively on host APCs[4,8], become activated and differentiate into various effector and memory T cells. For instance, donor $CD8^+$ T cells differentiate into anti-host CTLs and express cytotoxic molecules such as perforin, granzyme B and/or FasL[5,7,10,11]. Second, by the expression of tissue-specific adhesion and chemoattractant receptors, antigen-specific effector and memory T cells in general display selective tropism for specific peripheral tissues and infiltrate into all tissues in the body—especially the epithelial surface[7–9,12–15], in which a variety of tissue-specific adhesion molecules and chemokines are copiously expressed. Chemokine CCL3 (macrophage inflammatory protein 1α)-induced migration of CCR5-expressing $CD8^+$ T cells into liver has been implicated in liver injury associated with mouse a-GVHD[16]. In addition, a significant decrease in the quantitative assessment of a-GVHD in the liver after transfer of $CCL3^{-/-}$ splenocytes compared with $CCL3^{+/+}$ splenocytes has been reported[17].

Although these consecutive events occur during the progression of a-GVHD, much remains to be learned about their etiological significance and the key lymphoid compartment where donor-derived anti-host CTLs start to differentiate. By taking advantage of a well-characterized mouse acute graft-*versus*-host reaction (a-GVHR) model, namely, injection of parent C57BL/6 (B6; H-2^b) spleen cells into unirradiated (C57BL/6 × DBA/2)F1 (BDF1; H-$2^{b\times d}$) hosts[3,6,11,16,18,19], we performed anatomical and kinetic studies on the cellular and molecular events that lead to a-GVHD. Our results indicate that the subepithelial dome (SED) of gut Peyer's patches (PPs) is the pivotal anatomical site for the generation of anti-host CTLs and the resultant manifestation of a-GVHD. In two well-characterized, lethal a-GVHR models in which donor T cells were transferred into irradiated mice, host survival was prolonged in the progeny of transplacentally manipulated PP-deficient, but otherwise normal, recipient mice. Thus, infiltration of donor $CD8^+$ T cells into host PPs is of paramount importance for the induction of a-GVHD.

Results

Donor $CD8^+$ T cells infiltrate into SEDs of host PPs

First, we followed the trafficking of donor T cells in a well-characterized parent → F1 a-GVHR model[3,6,11,16,18,19]. Unirradiated BDF1 mice were injected with 5×10^7 splenocytes from parental B6 mice carrying enhanced green fluorescent protein ($eGFP^+$). eGFP expression is driven by the chicken β-actin promoter and a cytomegalovirus (CMV)

[1]Department of Molecular Preventive Medicine, Graduate School of Medicine, The University of Tokyo, Bunkyo-ku, Tokyo 113-0033, Japan. [2]Department of Internal Medicine, Niigata University School of Medicine, Niigata-shi, Niigata 951-8122, Japan. [3]Department of Anatomy & Developmental Biology, School of Medicine, Tokyo Women's Medical University, Shinjyuku-ku, Tokyo 162-8666, Japan. Departments of [4]Biochemistry and [5]Microbiology, School of Medicine, Keio University, Shinjyuku-ku, Tokyo 160-8582, Japan. Correspondence should be addressed to K.M. (koujim@m.u-tokyo.ac.jp).

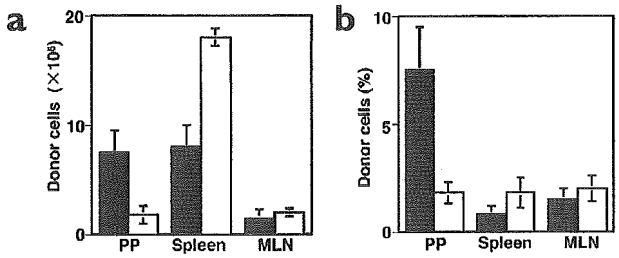

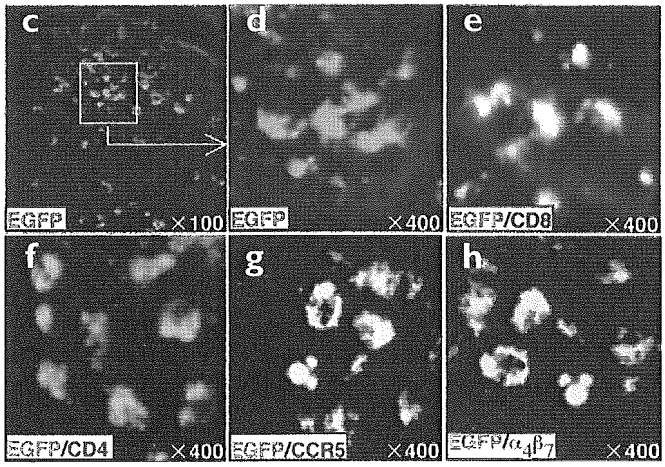

Figure 1. Early and prominent infiltration of donor CD8⁺ T cells into SED regions of host PPs. Shown are absolute numbers (**a**) and population size (**b**) (%) of donor CD8⁺ (filled bars) and CD4⁺ (open bars) T cells recovered from PPs, spleen and MLNs of host BDF1 mice on day 2 after injection with eGFP⁺ B6 spleen cells (n = 6). On day 2 after injection with eGFP⁺ B6 spleen cells, fluorescence and two-color immunofluorescence analyses were performed on the tissue sections of PP prepared from host BDF1 mice. (**c** and **d**) Fluorescence analysis shows that donor eGFP⁺ B6 cells (green) are congregating densely at SED regions of PPs. Donor eGFP⁺ cells congregating at SED regions of PPs were stained with CD8 mAb (PE) (**e**), with CD4 mAb (PE) (**f**), with mAb to chemokine receptor CCR5 (PE) (**g**) or with mAb to integrin $\alpha_4\beta_7$ (PE) (**h**). Overlapping fluorescence in the image appears in yellow.

immediate early enhancer. eGFP is expressed in all tissues except red blood cells and hair[20]. As a control, we used eGFP⁺ BDF1 splenocytes. On day 2 after injection, we examined the tissue sections and detected donor eGFP⁺ B6 cells in all lymphoid tissues of BDF1 hosts, including PPs, spleen, peripheral lymph nodes, blood, gut mucosa and liver (data not shown). To characterize the colonizing donor T cells precisely, we carried out flow cytometric analysis on lymphocytes isolated from PPs, spleen and mesenteric lymph nodes (MLNs). The numbers of lymphoid cells recovered were about 10^7 from PPs (ten PPs on average), about 10^8 from spleen and about 10^7 from MLNs. Although absolute numbers of donor eGFP⁺CD8⁺ T cells in PPs were almost comparable to those that localized to the spleen (7.5×10^5 cells), the percentage of the eGFP⁺CD8⁺ T cell population in PPs was far larger (by a factor of 7) than that in spleen, and such biased colonization was not observed in donor eGFP⁺CD4⁺ T cells (**Fig. 1a,b**). In contrast, few if any syngeneic eGFP⁺ donor BDF1 spleen cells were detected in host BDF1 PPs of the day 2 post-injection period (data not shown).

We further investigated this selective donor B6 CD8⁺ T cell migration into host BDF1 PPs. We noticed that eGFP⁺ cells were congregated just beneath the follicle-associated epithelium, namely, at the SED region of PPs (**Fig. 1c,d** and **Supplementary Fig. 1a,b** online). We next examined the cell surface molecules of eGFP⁺ cells. Unexpectedly, almost all eGFP⁺ cells expressed CD8 (**Fig. 1e**), whereas relatively fewer CD4⁺ cells were found in this location (**Fig. 1f**). These donor CD8⁺ cells also coexpressed a chemokine receptor CCR5 (**Fig. 1g**), and integrin $\alpha_4\beta_7$ (**Fig. 1h**). Although we did not explore the mechanism underlying this biased colonization of donor CD8⁺ over CD4⁺ T cells in the SED region of PP, we detected a substantial numbers of donor eGFP⁺CD4⁺ T cells in the follicular and parafollicular regions of host PP (data not shown).

Donor PP CD8⁺ T cells display anti-host cytotoxicity

By investigating the same mouse a-GVHR model, we previously showed that CCL3-mediated attraction of CCR5-expressing donor CD8⁺ T cells is critical in causing liver injury[16]. In this context, we determined the expression of chemokine ligands for CCR5, namely, CCL3, CCL4 (macrophage inflammatory protein-1β) and CCL5 (RANTES), in the SED region of host PPs. Based on the SED location, we expected that most chemokine-producing cells would be CD11c⁺ dendritic cells (DCs), which are prevalent in this area[21–23] (**Supplementary Fig. 1c** online), and that these DCs would attract CCR5-expressing donor CD8⁺ T cells. Indeed, by day 2 after injection, donor eGFP⁺CD8⁺ T cells from B6 mice were in close proximity with host DCs, which stained with anti-CD11c (**Fig. 2a**). CCL5 (RANTES) was expressed on such CD11c⁺ cells (**Fig. 2b**). In contrast to the expression of CCL5, other ligands for

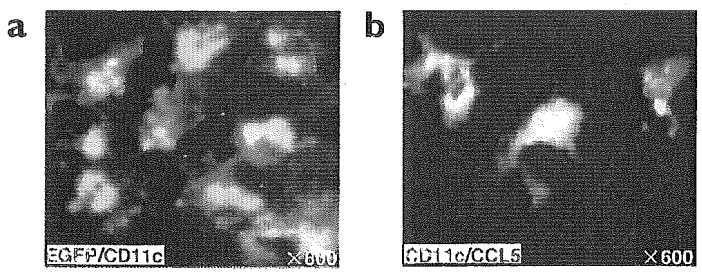

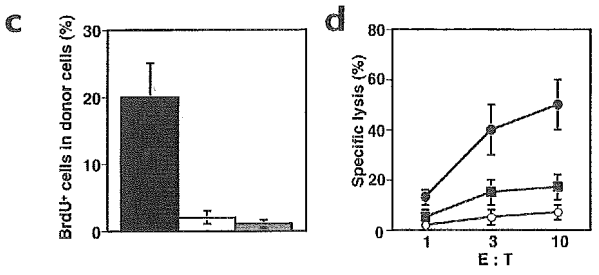

Figure 2. Characterization of donor CD8⁺ T cells that infiltrate into SED regions of host PPs. On day 2 after injection with eGFP⁺ B6 spleen cells, two-color immunofluorescence analysis was performed on the tissue sections of PP prepared from host BDF1 mice. (**a**) Interactions between donor eGFP⁺ cells (green) and CD11c⁺ cells (red) were visualized at SED regions of PPs. (**b**) High-magnification image of the SED region of PPs stained with CD11c mAb (FITC) and polyclonal CCL5 antibodies (Texas red). Overlapping fluorescence in the image appears in yellow. (**c**) Population size (%) of DNA-replicating donor eGFP⁺ cells recovered from PPs (filled bar), spleen (open bar) and MLNs (shaded bar) of BDF1 hosts on day 2 after injection (n = 4). (**d**) CTL activities of sorted donor CD8⁺ T cells from PPs of host BDF1 (H-$2^{b \times d}$) mice were determined to DBA/2 (H-2^d) (filled circles) and C3H/HeN (H-2^k) (open circles) splenic target cells on day 2 after injection with eGFP⁺ B6 (H-2^b) spleen cells (n = 7). CTL activity of sorted donor CD8⁺ T cells from spleen of host BDF1 (H-$2^{b \times d}$) mice to DBA/2 (H-2^d) (filled squares) splenic target cells was also determined on day 2 after injection with eGFP⁺ B6 (H-2^b) spleen cells (n = 7).

© 2003 Nature Publishing Group http://www.nature.com/natureimmunology

Research Fellowships of the Japan Society for the Promotion of Science for Young Scientists (M.M.), by Grant-in-Aid for Creative Scientific Research, the Japan Society for the Promotion of Science (13GS0015) and Special Coordination Fund for Promoting Science and Technology, Ministry of Education, Culture, Sport, Science and Technology (H.I.) and by a grant from Solution Oriented Research for Science and Technology (SORST), Japan Science and Technology Corporation (K.M.).

Competing interests statement

The authors declare that they have no competing financial interests.

Received 8 October 2002; accepted 2 December 2002.

© 2003 Nature Publishing Group http://www.nature.com/natureimmunology

1. Appelbaum, F.R. Haematopoietic cell transplantation as immunotherapy. *Nature* **411**, 385–389 (2001).
2. Ho, V.T. & Soiffer, R.J. The history and future of T-cell depletion as graft-*versus*-host disease prophylaxis for allogeneic hematopoietic stem cell transplantation. *Blood* **98**, 3192–3204 (2001).
3. Mowat, A.M. & Felstein, M.V. Experimental studies of immunologically mediated enteropathy. V. Destructive enteropathy during an acute graft-*versus*-host reaction in adult BDF1 mice. *Clin. Exp. Immunol.* **79**, 279–284 (1990).
4. Sprent, J. & Korngold, R. Murine models for graft-*versus*-host disease. in *Bone Marrow Transplantation* (eds. Forman, S.J., Blume, K.J. & Thomas, E.D.) 220–230 (Blackwell Scientific Publications, Boston, 1994).
5. Baker, B.M.B., Altman, N., Podack, E. & Levy, R.B. The role of cell-mediated cytotoxicity in acute GVHD after MHC-matched allogeneic bone marrow transplantation in mice. *J. Exp. Med.* **183**, 2645–2656 (1996).
6. Tamada, K. *et al.* Modulation of T-cell-mediated immunity in tumor and graft-*versus*-host disease models through the LIGHT co-stimulatory pathway. *Nat. Med.* **6**, 283–289 (2000).
7. Antin, J.H. Acute graft-versus-host disease: inflammation run amok? *J. Clin. Invest.* **107**, 1497–1498 (2001).
8. Shlomchik, W.D. *et al.* Prevention of graft-*versus*-host disease by inactivation of host antigen-presenting cells. *Science* **285**, 412–415 (1999).
9. Ferrara, J.L.M. & Deeg, H.J. Graft-*versus*-host disease. *N. Eng. J. Med.* **324**, 667–674 (1991).
10. Shustov, A., Nguyen, P., Finkelman, F., Elkeon, K.B. & Via, C.S. Differential expression of Fas and Fas ligand in acute and chronic graft-*versus*-host disease: up-regulation of Fas and Fas ligand requires $CD8^+$ T cell activation and IFN-γ production. *J. Immunol.* **161**, 2848–2855 (1998).
11. Lin, T. *et al.* Fas ligand-mediated killing by intestinal intraepithelial lymphocytes. *J. Clin. Invest.* **101**, 570–577 (1998).
12. Mackay, C.R. Dual personality of memory T cells. *Nature* **401**, 659–660 (1999).
13. Sallusto, F., Lenig, D., Forster, R., Lipp, M. & Lanzavecchia, A. Two subsets of memory T lymphocytes with distinct homing potentials and effector functions. *Nature* **401**, 708–712 (1999).
14. Kunkel, E.J. & Butcher, E.C. Chemokines and the tissue-specific migration of lymphocytes. *Immunity* **16**, 1–4 (2002).
15. Campbell, D.J. & Butcher, E.C. Rapid acquisition of tissue-specific homing phenotypes by $CD4^+$ T cells activated in cutaneous or mucosal lymphoid tissues. *J. Exp. Med.* **195**, 135–141 (2002).
16. Murai, M. *et al.* Active participation of $CCR5^+CD8^+$ T lymphocytes in the pathogenesis of liver injury in graft-*versus*-host disease. *J. Clin. Invest.* **104**, 49–57 (1999).
17. Serody, J.S. *et al.* T-lymphocyte production of macrophage inflammatory protein-1a is critical to the recruitment of CD8+ T cells to the liver, lung, and spleen during graft-*versus*-host disease. *Blood* **96**, 2973–2980 (2000).
18. Pals, S.T., Radaszkiewicz, T. & Gleichmann, E. Allosuppressor- and allohelper-T cells in acute and chronic graft-*versus*-host disease IV. Activation of donor allosuppressor cells is confined to acute GVHD. *J. Immunol.* **132**, 1669–1678 (1984).
19. Sakai, T., Ohara-Inagaki, K., Tsuzuki, T. & Yoshikai, Y. Host intestinal intraepithelial gd T lymphocytes present during acute graft-*versus*-host disease in mice may contribute to the development of enteropathy. *Eur. J. Immunol.* **25**, 87–91 (1995).
20. Okabe, M., Ikawa, M., Kominami, K., Nakanishi, T. and Nishimune, Y. 'Green mice' as a source of ubiquitous green cells. *FEBS Lett.* **407**, 313–319 (1997).
21. Kelsall, B.L. & Strober, W. Distinct populations of dendritic cells are present in the subepithelial dome and T cell regions of the murine Peyer's patch. *J. Exp. Med.* **183**, 237–247 (1996).
22. Banchereau, J. & Steinman, R.M. Dendritic cells and the control of immunity. *Nature* **392**, 245–252 (1998).
23. Iwasaki, A. & Kelsall, B.L. Freshly isolated Peyer's patch, but not spleen, dendritic cells produce interleukin 10 and induce the differentiation of T helper type 2 cells. *J. Exp. Med.* **190**, 229–239 (1999).
24. Yasmineh, W.G., Filipovich, A.H. & Killeen, A.A. Serum 5′ nucleotidase and alkaline phosphatase—highly predictive liver function tests for the diagnosis of graft-*versus*-host disease in bone marrow transplantation recipients. *Transplantation* **48**, 809–814 (1989).
25. Butcher, E.C., Williams, M., Youngman, K., Rott, L. & Briskin, M. Lymphocyte trafficking and regional immunity *Adv. Immunol.* **72**, 209–253 (1999).
26. Yoshida, H. *et al.* IL-7 receptor α^+ $CD3^-$ cells in the embryonic intestine induces the organizing center of Peyer's patches. *Int. Immunol.* **11**, 643–655 (1999).
27. Hamada, H. *et al.* Identification of multiple isolated lymphoid follicles on the antimesenteric wall of the mouse small intestine. *J. Immunol.* **168**, 57–64 (2002).
28. Korngold, R. & Sprent, J. T-cell subsets in graft-*versus*-host disease. in *Graft- versus-Host Disease: Immunology, Pathophysiology and Treatment* (eds. Burakoff, S.J., Deeg, H.J., Ferrara, J.L.M. & Atkinson, K.) 31–50 (Marcel Dekker, New York, 1990).
29. Tamada, K. *et al.* Blockade of LIGHT/LTβ and CD40 signaling induces allospecific T cell anergy, preventing graft-*versus*-host disease. *J. Clin. Invest.* **109**, 549–557 (2002).
30. Sprent, J. Fate of H2-activated T lymphocytes in syngeneic hosts I. Fate in lymphoid tissues and intestines traced with ^{3}H-Thymidine, ^{125}I-Deoxyuridine and ^{51}Chromium. *Cell. Immunol.* **21**, 278–302 (1976).
31. Sprent, J. & Miller, J.F.A.P. Interaction of thymus lymphocytes with histocompatible cells. II. Recirculating lymphocytes derived from antigen-activated thymus cells. *Cell. Immunol.* **3**, 385–404 (1972).
32. Sprent, J. & Miller, J.F.A.P. Interaction of thymus lymphocytes with histocompatible cells. I. Quantitation of the proliferative response of thymus cells. *Cell. Immunol.* **3**, 361–384 (1972).
33. Gebert, A., Rothkotter, H.J. & Pabst, R. M cells in Peyer's patches of the intestine. *Int. Rev. Cytol.* **167**, 91–159 (1996).
34. Neutra, M.R., Mantis, N.J. & Kraehenbuhl, J.-P. Collaboration of epithelial cells with organized mucosal lymphoid tissues. *Nat. Immunol.* **2**, 1004–1009 (2001).
35. Hurst, S.D., Sitterding, S.M., Ji, S. & Barrett, T.A. Functional differentiation of T cells in the intestine of T cell receptor transgenic mice. *Proc. Natl. Acad. Sci. USA* **94**, 3920–3925 (1997).
36. MacDonald, T. Introduction. *Semin. Immunol.* **13**, 159–161 (2001).
37. Elson, C.O., Cong, Y., Iqbal, N. & Weaver, C.T. Immuno-bacterial homeostasis in the gut: new insight into an old enigma. *Semin. Immunol.* **13**, 187–194 (2001).
38. Simmons, C.P., Clare, S. & Dougan, G. Understanding mucosal responsiveness: lessons from enteric bacterial pathogens. *Semin. Immunol.* **13**, 201–209 (2001).
39. Weinstein, P.D. & Cebra, J.J. The preference for switching to IgA expression by Peyer's patch germinal center B cells is likely due to the intrinsic influence of their microenvironment. *J. Immunol.* **147**, 4126–4135 (1991).
40. Sudo, N. *et al.* The requirement of intestinal bacterial flora for the development of an IgE production system fully susceptible to oral tolerance induction. *J. Immunol.* **159**, 1739–1745 (1997).
41. Singh, B. *et al.* Control of intestinal inflammation by regulatory T cells. *Immunol. Rev.* **182**, 190–200 (2001).
42. Vossen, J.M. & Heidt, P.J. Gnotobiotic measures for the prevention of acute graft-versus-host disease. in *Graft-versus-Host Disease: Immunology, Pathophysiology and Treatment* (eds. Burakoff, S.J., Deeg, H.J., Ferrara, J.L.M. & Atkinson, K.) 403–413 (New York, Marcel Dekker, 1990).
43. Nestle, F.P., Price, K.S., Seemayer, T.A. and Lapp, W.S. Macrophage priming and lipopolysaccharide-triggered release of tumor necrosis factor α during graft-*versus*-host disease. *J. Exp. Med.* **175**, 405–413 (1992).
44. Cooke, K.R. *et al.* Tumor necrosis factor-α production to lipopolysaccharide stimulation by donor cells predicts the severity of experimental acute graft-*versus*-host disease. *J. Clin. Invest.* **102**, 1882–1891 (1998).
45. Cooke, K.R. *et al.* LPS antagonism reduces graft-*versus*-host disease and preserves graft-*versus*-leukemia activity after experimental bone marrow transplantation. *J. Clin. Invest.* **107**, 1581–1589 (2001).
46. Dazzi, F., Simpson, E. & Goldman, J.M. Minor antigen solves major problem. *Nat. Med.* **7**, 769–770 (2001).
47. Garside, P. & Mowat, A.M. Oral tolerance. *Semin. Immunol.* **13**, 177–185 (2001).
48. Decker, T. & Lohmann-Matthes, M.L. A quick and simple method for the quantitation of lactate dehydrogenese release in mesasurements of cellular cytotoxicity and tumor necrosis factor (TNF) activity. *J. Immunol. Methods* **115**, 61–69 (1988).
49. Yoneyama, H. *et al.* Regulation by chemokines of circulating dendritic cell precursors, and the formation of portal tract-associated lymphoid tissue, in a granulamatous liver disease. *J. Exp. Med.* **193**, 35–49 (2001).

Peyer's patch is the essential site in initiating murine acute and lethal graft-*versus*-host reaction

Masako Murai, Hiroyuki Yoneyama, Taichi Ezaki, Makoto Suematsu, Yuya Terashima, Akihisa Harada, Hiromasa Hamada, Hitoshi Asakura, Hiromichi Ishikawa and Kouji Matsushima

Nature Immunology 4, 154–160 (2003).

In the February 2003 issue of *Nature Immunology*, incorrect versions of panels e and h of Figure 1 and panels d and e of Figure 6 were supplied and printed. The correct panels are printed below. This mistake does not affect the message of the paper.

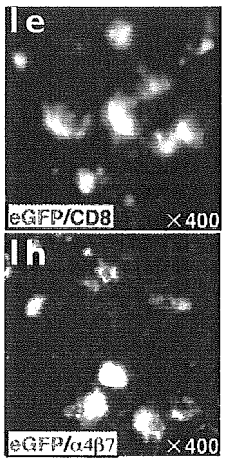

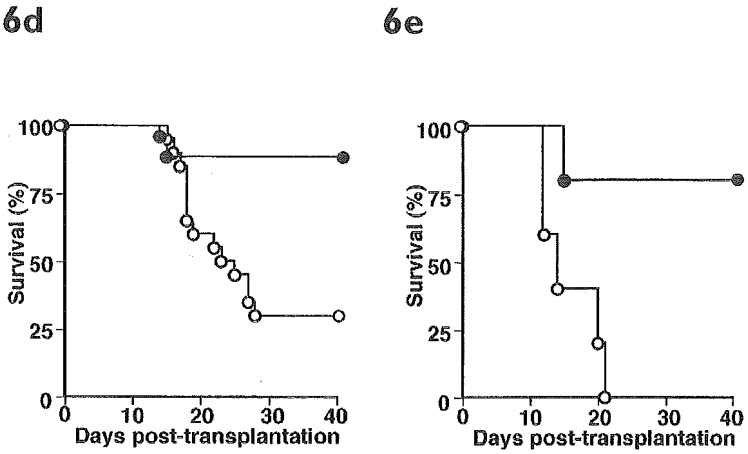

© 2003 Nature Publishing Group http://www.nature.com/natureimmunology